AD-A040 002 ARMY ELECTRONICS COMMAND FORT MONMOUTH N J F/G 20/3
A THEORY OF SCATTERING BY SINUSOIDAL METAL SURFACES.(U)
MAY 77 F SCHWERING, G WHITMAN

UNCLASSIFIED ECOM-4496 NL

| OF |
AD
A040 002

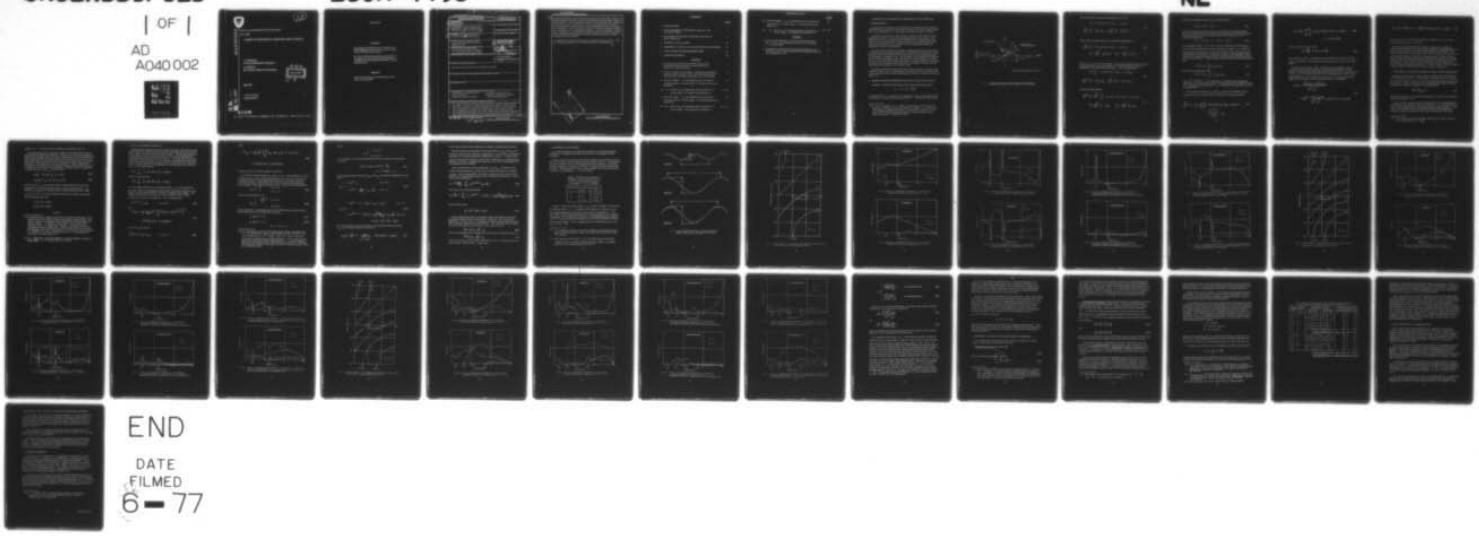

END

DATE
FILMED
6-77

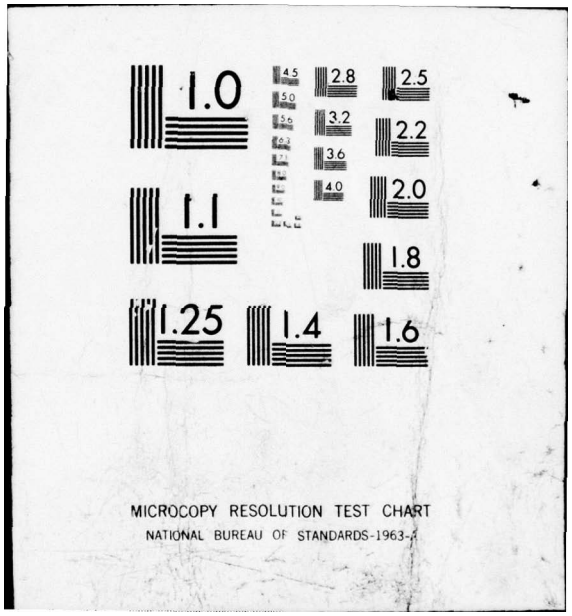
1.0
1.1
1.25
1.4
1.6
1.8
2.0
2.2
2.5
2.8
3.2
3.6
4.0
4.5
5.0
5.6
6.3
7.1
MICROCOPY RESOLUTION TEST CHART
NATIONAL BUREAU OF STANDARDS-1963-A

(12)

Research and Development Technical Report

ECOM-4496

A THEORY OF SCATTERING BY SINUSOIDAL METAL SURFACES

F. Schwering
Communications/ADP Laboratory

G. Whitman
New Jersey Institute of Technology

May 1977

DISTRIBUTION STATEMENT

Approved for public release;
distribution unlimited.

ECOM

US ARMY ELECTRONICS COMMAND FORT MONMOUTH, NEW JERSEY 07703

NOTICES

Disclaimers

The findings in this report are not to be construed as an official Department of the Army position, unless so designated by other authorized documents.

The citation of trade names and names of manufacturers in this report is not to be construed as official Government indorsement or approval of commercial products or services referenced herein.

Disposition

Destroy this report when it is no longer needed. Do not return it to the originator.

(9) Research and development technical rept.,

UNCLASSIFIED

SECURITY CLASSIFICATION OF THIS PAGE (When Data Entered)

REPORT DOCUMENTATION PAGE

READ INSTRUCTIONS BEFORE COMPLETING FORM

(14) REPORT NUMBER: ECOM-4496

2. GOVT ACCESSION NO.

3. RECIPIENT'S CATALOG NUMBER

4. TITLE (and Subtitle)

(6) A THEORY OF SCATTERING BY SINUSOIDAL METAL SURFACES

5. TYPE OF REPORT & PERIOD COVERED

6. PERFORMING ORG. REPORT NUMBER

7. AUTHOR(s)

(10) F. Schwering and G. Whitman

8. CONTRACT OR GRANT NUMBER(s)

9. PERFORMING ORGANIZATION NAME AND ADDRESS

Communications/ADP Laboratory
DRSEL-NL-RH
Fort Monmouth, New Jersey 07703

10. PROGRAM ELEMENT, PROJECT, TASK AREA & WORK UNIT NUMBERS

(16) 1T1 61102 B31A 01 451

(17)

11. CONTROLLING OFFICE NAME AND ADDRESS

Communications/ADP Laboratory
U. S. Army Electronics Command
Fort Monmouth, New Jersey 07703

12. REPORT DATE

(11) May 1977

13. NUMBER OF PAGES

35 (12) 41p.

14. MONITORING AGENCY NAME & ADDRESS (if different from Controlling Office)

15. SECURITY CLASS. (of this report)

UNCLASSIFIED

15a. DECLASSIFICATION/DOWNGRADING SCHEDULE

16. DISTRIBUTION STATEMENT (of this Report)

Approved for public release; distribution unlimited

17. DISTRIBUTION STATEMENT (of the abstract entered in Block 20, if different from Report)

18. SUPPLEMENTARY NOTES

19. KEY WORDS (Continue on reverse side if necessary and identify by block number)

Scattering by periodic surfaces;
Space harmonics;
Extended boundary condition;
Microwave landing systems;
Dependence of specular reflected power on polarization.

20. ABSTRACT (Continue on reverse side if necessary and identify by block number)

A rigorous theory of plane wave scattering by periodic metal surfaces is presented. The physical optics approximation is used to determine the current distribution on the metal surface to first order, but this approximate distribution is modified by multiplication with a Fourier series, whose fundamental period is that of the surface profile (Floquet's theorem). The coefficients of the Fourier series are determined by invoking the condition that the field radiated by the current distribution into the lower

→ next page

DD FORM 1 JAN 73 1473 EDITION OF 1 NOV 65 IS OBSOLETE

UNCLASSIFIED

SECURITY CLASSIFICATION OF THIS PAGE (When Data Entered)

CDE 037620

cont →

(shielded) half-space cancels the primary plane wave in this space range. The scatter problem is thereby reduced to the familiar task of solving a system of linear equations. For certain basic types of surface profiles, the coefficients of the linear system are obtained in closed form (Bessel functions for the sinusoidal profiles considered here, and exponential functions for piecewise linear profiles). Thus, the method requires no numerical integral evaluation and, consequently, is computationally efficient. Since the boundary condition of zero tangential electric field at the metal surface is not utilized, the field within the grooves of the periodic scatterer need not be known--a definite advantage of the new method.

In addition to a summary of the theory, numerical results for TE-, TM-, and circular polarization of the incident plane wave are presented.

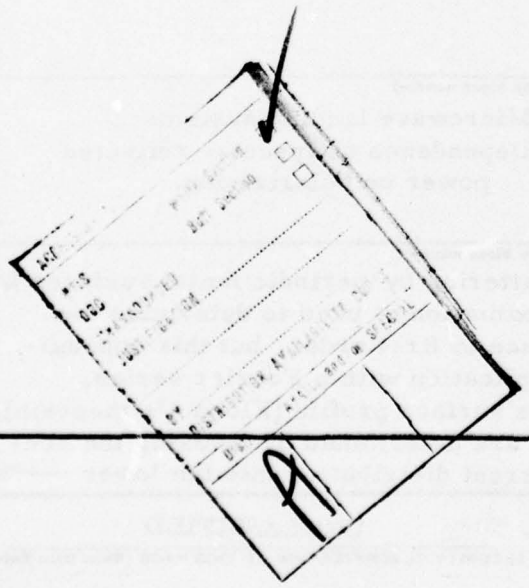

CONTENTS

FIGURES

CONTENTS (Contd.)

TABLES

A THEORY OF SCATTERING BY SINUSOIDAL METAL SURFACES

1. INTRODUCTION

The problem of scattering by periodically-corrugated metal surfaces is analyzed using an approach which extends the physical optics approximation into a rigorous theory and is amenable to efficient computer evaluation.

The theory was derived in the course of a study of the much discussed polarization problem of microwave landing systems. One aspect of this problem concerns scattering by large periodic metal surfaces near runways--such as hangar doors--and the question as to whether the specular reflection coefficient of such surfaces can be significantly reduced by appropriate choice of polarization.

Numerical data obtained by computer evaluation of the theory show that horizontal polarization generally leads to substantially less specular reflection than does vertical polarization, particularly in the interesting range of low angles of incidence, i.e., near grazing. (It is implied here that the grooves of the corrugated surface run in the vertical direction.) Furthermore, it was found that circular polarization is highly effective in suppressing higher order grating lobes of the same polarization (circular with the same sense of rotation) as the incident wave.

A detailed presentation of the new theory will be given in a forthcoming technical report. For a comprehensive literature survey of previous work in the field of periodic surface scattering, we refer to a report by Tong and Senior [1].

2. SPACE HARMONICS REPRESENTATION OF THE SCATTER FIELD

Consider a periodic metal surface with a sinusoidal height profile

$$z_0 = h \sin\left(2\pi \frac{x_0}{d}\right) \qquad (1)$$

as shown in Fig. 1. A plane wave of dependence $\exp(i\omega t)$ and amplitude E^P is assumed to be incident from the direction θ. For the TE-polarization

---

[1] T. C-H. Tong and T. B. A. Senior, "Scattering of electromagnetic waves by a periodic surface with arbitrary profile," The University of Michigan, Scientific Report No. 13, April 1972, Prepared for Air Force Cambridge Research Laboratories, Bedford, Mass. 01730, under Contract No. F19628-68-C-0071.

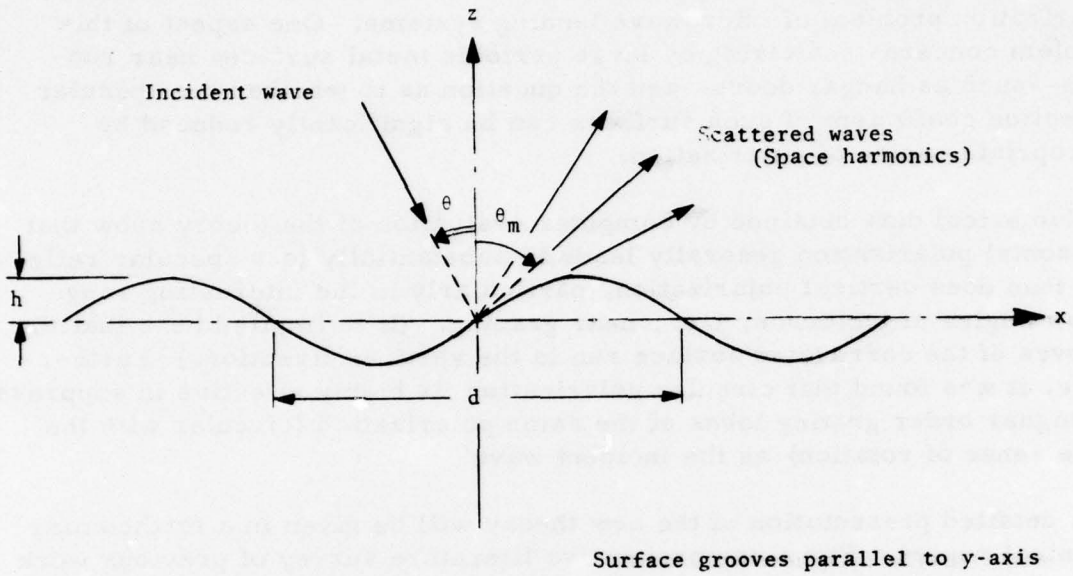

Fig. 1. Periodic metal surface illuminated by plane wave: Coordinates and geometrical parameters used in analysis of scatter problem.

case, the field components of the primary wave are

$$E_y^P = +E^P \exp(-ik\,(x\sin\theta - z\cos\theta))$$

$$\sqrt{\frac{\mu}{\varepsilon}}\,H_x^P = +E_y^P\cos\theta\ ,\quad \sqrt{\frac{\mu}{\varepsilon}}\,H_z^P = +E_y^P\sin\theta \tag{2a}$$

and for the TM-polarization case, the field components are

$$\sqrt{\frac{\mu}{\varepsilon}}\,H_y^P = +E^P \exp(-ik(x\sin\theta - z\cos\theta)) \tag{2b}$$

$$E_x^P = -\sqrt{\frac{\mu}{\varepsilon}}\,H_y^P\cos\theta,\qquad E_z^P = -\sqrt{\frac{\mu}{\varepsilon}}\,H_y^P\sin\theta\ ,$$

where $k = 2\pi/\lambda$ is the wave number. Due to the periodicity of the surface, the scatter field can be represented as a discrete spatial spectrum of propagating and evanescent plane waves. For TE-polarization

$$E_y^S = \sum_{m=-\infty}^{+\infty} E_m \exp(-ik(x\sin\theta_m + z\cos\theta_m))$$

$$\sqrt{\frac{\mu}{\varepsilon}}\,H_x^S = -E_y^S\cos\theta_m,\quad \sqrt{\frac{\mu}{\varepsilon}}\,H_z^S = +E_y^S\sin\theta_m\ , \tag{3a}$$

and for TM-polarization

$$\sqrt{\frac{\mu}{\varepsilon}}\,H_y^S = \sqrt{\frac{\mu}{\varepsilon}}\sum_{m=-\infty}^{+\infty} H_m \exp(-ik(x\sin\theta_m + z\cos\theta_m))$$

$$E_x^S = +\sqrt{\frac{\mu}{\varepsilon}}\,H_y^S\cos\theta_m,\qquad E_z^S = -\sqrt{\frac{\mu}{\varepsilon}}\,H_y^S\sin\theta_m\ , \tag{3b}$$

where the propagation angles θ_m are determined by

$$\sin\theta_m = \sin\theta + m\frac{\lambda}{d} \quad . \tag{4a}$$

Apart from the common phase factor exp {-ikxsin θ}, all of these plane waves are periodic with d, the groove width of the metal surface (Floquet's theorem); they have therefore been called "space harmonics." For m-values in the range

$$-\frac{d}{\lambda}(1 + \sin\theta) < m < +\frac{d}{\lambda}(1 - \sin\theta), \tag{4b}$$

the propagation angles θ_m are real, and the associated space harmonics are of the propagating type; for the remaining m-values, θ_m is complex, and the space harmonics are of the evanescent type, that is, they decrease exponentially in the positive z-direction. Clearly, only propagating space harmonics transmit real power, while evanescent space harmonics exhibit purely reactive power. Conservation of energy requires for TE-polarization that

$$E^P \cdot E^{P*} \cos\theta = \sum_{m_1}^{m_2} E_m \cdot E_m^* \cos\theta_m \tag{5a}$$

and for TM-polarization that

$$H^P \cdot H^{P*} \cos\theta = \sum_{m_1}^{m_2} H_m \cdot H_m^* \cos\theta_m \tag{5b}$$

where $H^P = \sqrt{\varepsilon/\mu}\, E^P$. The summations are limited to the propagating spectral orders defined by Eq. (4b). The space harmonic of spectral order m = 0 propagates in the direction $\theta_0 \approx \theta$ and hence is termed the "specular reflected wave."

The complex amplitudes E_m and H_m of the space harmonics can be expressed in terms of the current distribution on the metal surface:

$$\sqrt{\frac{\varepsilon}{\mu}}\, E_m = -\frac{1}{2d} \int_{x_0=-d/2}^{x_0=+d/2} I_y(x_0) \exp\{ik(x_0 \sin\theta_m + z_0 \cos\theta_m)\} \times \tag{6a}$$

$$\times \frac{\sqrt{1 + z_0'^2}}{\cos\theta_m}\, dx_0$$

$$H_m = + \frac{1}{2d} \int_{x_0=-\frac{d}{2}}^{x_0=+\frac{d}{2}} I_{x,z}(x_0) \exp\{ik(x_0 \sin\alpha_m + z_0 \cos\alpha_m)\} \times \qquad (6b)$$

$$\times (1 - z_0' \operatorname{tg} \alpha_m) dx_0$$

where z_0 is given by Eq. (1) and

$$z_0' = \frac{dz_0}{dx_0} = 2\pi \frac{h}{d} \cos\left(2\pi \frac{x_0}{d}\right) . \qquad (6c)$$

The symbols I_y and $I_{x,z}$ denote the current densities in the TE- and TM-cases, respectively. The integrations extend over one period of the metal surface.

If this surface period is large compared to a wavelength, it may be assumed that the current densities are determined primarily by local effects, and the physical optics approximation may be used. In other words, I_y and $I_{x,z}$ at each surface element may be approximated by the currents which would flow in the element if it were part of an infinite metal plane tangent to the surface z_0 at the element location. Accordingly,

$$I_y(x_0) \approx +2 \frac{H_x^P(x_0,z_0) + z_0' H_z^P(x_0,z_0)}{\sqrt{1 + z_0'^2}} \qquad (7a)$$

$$= +2\sqrt{\frac{\varepsilon}{\mu}} E^P \frac{\cos\theta + z_0' \sin\theta}{\sqrt{1 + z_0'^2}} \exp\left(-ik(x_0 \sin\theta - z_0 \cos\theta)\right)$$

$$I_{x,z}(x_0) \approx -2H_y^P(x_0,z_0) = -2\sqrt{\frac{\varepsilon}{\mu}}\, E^P \exp(-ik(x_0 \sin\theta - z_0 \cos\theta)) \qquad (7b)$$

where z_0 and z_0' are the height and slope, respectively, of the surface profile as given by Eqs. (1) and (6c).

Inserting (7a) and (7b) into (6a) and (6b), respectively, results in explicit expressions for the scatter field amplitudes. Shadowing effects can be taken into account by using the current densities (7a) and (7b) in the directly illuminated surface regions only, while setting I_y and $I_{x,z}$ to zero in the shadow regions. Numerical evaluations show, however, that the physical optics approximation does not necessarily lead to results of sufficient accuracy even when the surface period d is of the order of several wavelengths. Large errors occur, particularly when the direction of arrival approaches grazing incidence ($\theta \to 90^0$). Hence, to obtain reliable results, rigorous solution of the scatter problem is required.

3. SOLUTION OF SCATTER PROBLEM (OUTLINE OF NEW APPROACH)

Rigorous solution of the scatter problem requires exact calculation of the amplitudes E_m and H_m. Unfortunately, the space harmonic representations (3a) and (3b) do not necessarily converge in the space ranges within the grooves. Hence, in general, these representations cannot be used to formulate the boundary condition at the metal surface

$$(\underline{E}^P + \underline{E}^S)_{tang} = 0 \qquad (8)$$

which would provide a straightforward approach to solution of the problem (Rayleigh's method) [2].

In recent years, several rigorous methods have been developed based on alternate representations of the scatter field, i.e., on representations which remain valid for the space range within the surface grooves. Typically, these methods utilize condition (8) and lead to inhomogeneous Fredholm integral equations for the current distribution on the metal

---

[2] For a discussion of the Rayleigh method and its range of validity, see Tong and Senior [1], page 1.

surface [3]. A survey of these methods can be found in Ref. [1].

In the present report, a rigorous method is described which does not use boundary condition (8) explicitly. Instead, the current distribution is found by formulating a space harmonic representation for the (hypothetical) field radiated into the half-space below the current-carrying surface and then postulating that this field cancels the primary plane wave in the lower half-space. This approach, which is related to a method suggested by Waterman for the analysis of scattering by bodies of finite dimensions [4], is outlined in more detail in the following. The first step is to expand the current densities I_y and $I_{x,z}$ into the series

$$I_y(x_0) = \hat{I}_y(x_0) \sum_n a_n f_n(x_0) \tag{9a}$$

$$I_{x,z}(x_0) = \hat{I}_{x,z}(x_0) \sum_n b_n g_n(x_0), \tag{9b}$$

where $\hat{I}_y$ and $\hat{I}_{x,z}$ are the physical optics approximations (7a) and (7b), respectively, or suitable modifications of these approximations. The functions f_n and g_n are assumed to form complete systems in the range $-d/2 \leq x_0 \leq d/2$. To satisfy Floquet's theorem for periodic structures, they must be periodic in d:

$$f_n(x_0 + d) = f_n(x_0)$$

$$g_n(x_0 + d) = g_n(x_0)$$

for all n

---

[3] An exception is an elegant recent theory by Hessel and Shmoys, which applies to periodic surfaces having a rectangular height profile. This theory employs a (waveguide) mode expansion for the field within the surface grooves. A summary of this theory can be found in the following report: A. Hessel and J. Shmoys, "Computer analysis of propagation/reflection phenomena," Polytechnic Institute of Brooklyn (Farmingdale, New York), Final Report, 20 August 1973 under Contract No. DAAB07-73-M-2716, Prepared for the U. S. Army Electronics Command, Fort Monmouth, N. J.

[4] P. C. Waterman, "Matrix formulation of electromagnetic scattering," Proc. IEEE, vol. 53, August 1965, pp. 805-812.

a_n and b_n are (unknown) coefficients.

Suppose these coefficients are not chosen correctly. Then the currents (9a) and (9b) will radiate a field not only into the half-space above the periodic surface, but also into the half-space below. (We assume temporarily that the metal surface is removed, but that the current distribution is maintained in place and that the half-space $z < 0$ has the same free-space properties as the half-space $z > 0$). Similar to the field in the upper half-space, the field in the lower half-space can be represented as a superposition of space harmonics propagating (or evanescing) away from the surface. For TE-polarization

$$E_y^T = \sum_{m=-\infty}^{+\infty} \bar{E}_m \exp(-ik(x \sin\theta_m - z\cos\theta_m))$$

and for TM-polarization

$$H_y^T = \sum_{m=-\infty}^{+\infty} \bar{H}_m \exp(-ik(x \sin\theta_m - z\cos\theta_m)) .$$

As in the upper half-space, the direction angles θ_m are determined by Eq. (4a). Hence, the propagation directions of the space harmonics in the upper and lower half-spaces are related by imaging at the z-plane. The complex amplitudes $\bar{E}_m$ and $\bar{H}_m$ are linear functions of the current coefficients a_n and b_n, respectively. For TE-polarization

$$\bar{E}_m = E^P \sum_n a_n U_{mn} \quad , \quad -\infty \le m \le +\infty \tag{10a}$$

with

$$E^P U_{mn} = -\frac{1}{2d} \frac{1}{\cos\theta_m} \sqrt{\frac{\mu}{\varepsilon}} \int_{-\frac{d}{2}}^{+\frac{d}{2}} \hat{I}_y(x_0) f_n(x_0) \sqrt{1 + z_0'^2} \times$$

$$\times \exp\{ik(x_0 \sin\theta_m - z_0 \cos\theta_m)\} dx_0 ; \tag{11a}$$

and for TM-polarization

$$\sqrt{\frac{\mu}{\varepsilon}}\, \bar{H}_m = E^P \sum_n b_n V_{mn} \quad , \quad -\infty \le m \le +\infty \tag{10b}$$

with

$$E^P V_{mn} = + \frac{1}{2d}\sqrt{\frac{\mu}{\varepsilon}} \int_{-\frac{d}{2}}^{+\frac{d}{2}} \hat{I}_{x,z}(x_0)\, g_n(x_0)\, (1 + z_0' \operatorname{tg}\theta_m) \times \tag{11b}$$

$$\times \exp\{ik(x_0 \sin\theta_m - z_0 \cos\theta_m)\}dx_0 .$$

where z_0 and z_0' are given by Eqs. (1) and (6c).

The correct current densities I_y and $I_{x,z}$, i.e., those flowing in a metal-surface, are now found by postulating that the field in the lower half-space is identically zero. This requires that the zero-order space harmonic cancels the primary wave (both waves travel in the same direction) and that all higher-order space harmonics vanish. Hence for TE-polarization

$$\bar{E}_m = \begin{cases} -E^P & \text{for } m = 0 \\ 0 & \text{for } m \neq 0 \end{cases} ; \tag{12a}$$

and for TM-polarization [5]

$$\bar{H}_m = \begin{cases} -\sqrt{\frac{\varepsilon}{\mu}}\, E^P & \text{for } m = 0 \\ 0 & \text{for } m \neq 0 \end{cases} . \tag{12b}$$

These equations in combination with (10a) and (10b) lead to linear systems for the unknown current coefficients a_n and b_n:

$$\sum_n U_{mn} a_n = -\delta_m \tag{13a}$$

$$\sum_n V_{mn} b_n = -\delta_m \tag{13b}$$

$$\text{for } -\infty \leq m \leq +\infty$$

---

[5] It is interesting to note that use of the physical optics approximation, i.e., the approximate current densities (7a) and (7b), results in zero order amplitudes $\bar{E}_0 = -E^P$ and $\bar{H}_0 = -\sqrt{\varepsilon/\mu}\, E^P$, which satisfy the zero order conditions (12a) and (12b) rigorously. This is true for both versions of the physical optics approximation, i.e., when shadowing effects are taken into account, and when they are neglected. However, the amplitudes of higher-order space harmonics do not generally vanish in this approximation.

where

$$\delta_m = \begin{cases} 1 \text{ for } m = 0 \\ 0 \text{ for } m \neq 0 \end{cases} .$$

It is expedient to choose the exponential Fourier system for the functions f_n and g_n

$$f_n(x_0) = g_n(x_0) = \exp\left(i2\pi n \frac{x_0}{d}\right) \qquad (14)$$

$$-\infty \leq n = \text{integer} \leq +\infty$$

The integrals (11a) and (11b) for U_{mn} and V_{mn} can then be evaluated in closed form

$$U_{mn} = \begin{cases} (-1)^{n+1} \delta_n & \text{for } m = 0 \\ (-1)^{n+m+1} \frac{\cos\theta}{\cos\theta_m} J_{m+n}(\bar{\beta}_m) & \text{for } m \neq 0 \end{cases} \qquad (15a)$$

$$V_{mn} = \begin{cases} (-1)^{n+1} \left[\delta_n - \pi \frac{h}{d} \operatorname{tg}\theta \, (\delta_{n+1} + \delta_{n-1})\right] & \text{for } m = 0 \\ (-1)^{m+n+1} \left[1 - \frac{\lambda}{d}(m+n) \frac{\operatorname{tg}\theta_m}{\cos\theta - \cos\theta_m}\right] J_{m+n}(\bar{\beta}_m) & \text{for } m \neq 0 \end{cases} \qquad (15b)$$

$$\text{with } \bar{\beta}_m = 2\pi \frac{h}{\lambda} (\cos\theta - \cos\theta_m)$$

In the evaluation, the physical optics current density (7b) was used for $\hat{I}_{x,z}$ and a modified version of (7a) for $\hat{I}_y$:

$$\hat{I}_y(x_0) = 2\sqrt{\frac{\varepsilon}{\mu}} \, E^P \, \frac{\cos\theta}{\sqrt{1 + z_0'^2}} \exp(-ik(x_0 \sin\theta - z_0 \cos\theta)) . \qquad (16)$$

It has been found that this modification enhances computational accuracy.

The incorporation of expressions (15a) and (15b) for U_{mn} and V_{mn} into the linear systems (13a) and (13b), respectively, permits efficient computer evaluation of the unknown Fourier coefficients a_n and b_n. A matrix inversion (or equivalent procedure) coupled with a routine for calculating Bessel functions of complex argument are required, but no time-consuming numerical integrations are needed.

After computing the current coefficients a_n and b_n, calculation of the scatter field amplitudes E_m and H_m for the upper half-space is straightforward. Upon inserting Eqs. (9a), (9b), and (14) into Eqs. (6a) and (6b), integrals are obtained which again can be evaluated in closed form. In the case of TE-polarization

$$E_m = E^P \frac{\cos\theta}{\cos\theta_m} \sum_{n=-\infty}^{+\infty} a_n (-1)^{m+n+1} J_{m+n}(\beta_m) \; ; \tag{17a}$$

and in the case of TM-polarization

$$H_m = -\sqrt{\frac{\epsilon}{\mu}}\, E^P \sum_{n=-\infty}^{+\infty} b_n (-1)^{m+n+1} \left[1 + \frac{\lambda}{d}(m+n)\frac{\operatorname{tg}\theta_m}{\cos\theta + \cos\theta_m}\right] J_{m+n}(\beta_m) \tag{17b}$$

where in both cases

$$\beta_m = 2\pi \frac{h}{\lambda} (\cos\theta + \cos\theta_m) \; . \tag{17c}$$

If the incident plane wave is circularly rather than linearly polarized, the space harmonics of the scatter field, in general, will be polarized elliptically. In this case, it is convenient to split the space harmonics into their circularly polarized component waves. The amplitude of the component wave rotating in the same sense as the incident wave is

$$E_m^{CS} = \frac{1}{2}\left(E_m + \sqrt{\frac{\mu}{\epsilon}}\, H_m\right) \; , \tag{18a}$$

while the amplitude of the component wave rotating in the opposite sense is

$$E_m^{CO} = \frac{1}{2}\left(E_m - \sqrt{\frac{\mu}{\epsilon}}\, H_m\right) \; , \tag{18b}$$

where E_m and H_m are the scatter amplitudes for TE- and TM-polarization given by Eqs. (17a) and (17b), respectively.

4. NUMERICAL EVALUATION

A computer program for numerical evaluation of the theory has been written [6]; evaluations have been performed on a Burroughs B-5500 Computer.

Numerical data was obtained for surface profiles of actual hangar doors. Full-scale traces of three such profiles are shown in Fig. 2. It is apparent that these profiles can be closely approximated by sinusoids, where only Profile 3 requires a moderate correction, as indicated by the dashed lines. In Table 1, the parameters d and h of these profiles are listed normalized relative to a wavelength of λ = 6 cm (C-band).

Table 1. Period d and Amplitude h of Surface Profiles Shown in Fig. 2; d and h are normalized relative to a wavelength λ = 6 cm (C-band).

Profile No.	Surface Parameters	
	d/λ	h/λ
1	1.3	0.1333
2	2.5	0.375
3	2.25	0.417

Figure 3 shows the scatter angles θ_m of surface Profile 1 as a function of incidence angle θ [7]. In Figures 4a through 7b, the powers P_m of the (propagating) space harmonics of this surface are plotted vs. θ for TE-, TM-, and circular polarization of the incident plane wave. Figures 8 through 12b and 13 through 17b show the corresponding data for Profiles 2 and 3. P_m is the power transmitted by the m^{th} space harmonic through unit area of a plane z = const. supposing that the incident power per unit area is unity. Thus

---

[6] The computer program is based on a slightly modified theory using sine and cosine functions, rather than exponential Fourier functions for f_n and g_n.

[7] Note that the scatter angles θ_m are counted positive in the first quadrant of the x, z-plane, while the incidence angle θ is counted positive in the second quadrant (see Fig. 1).

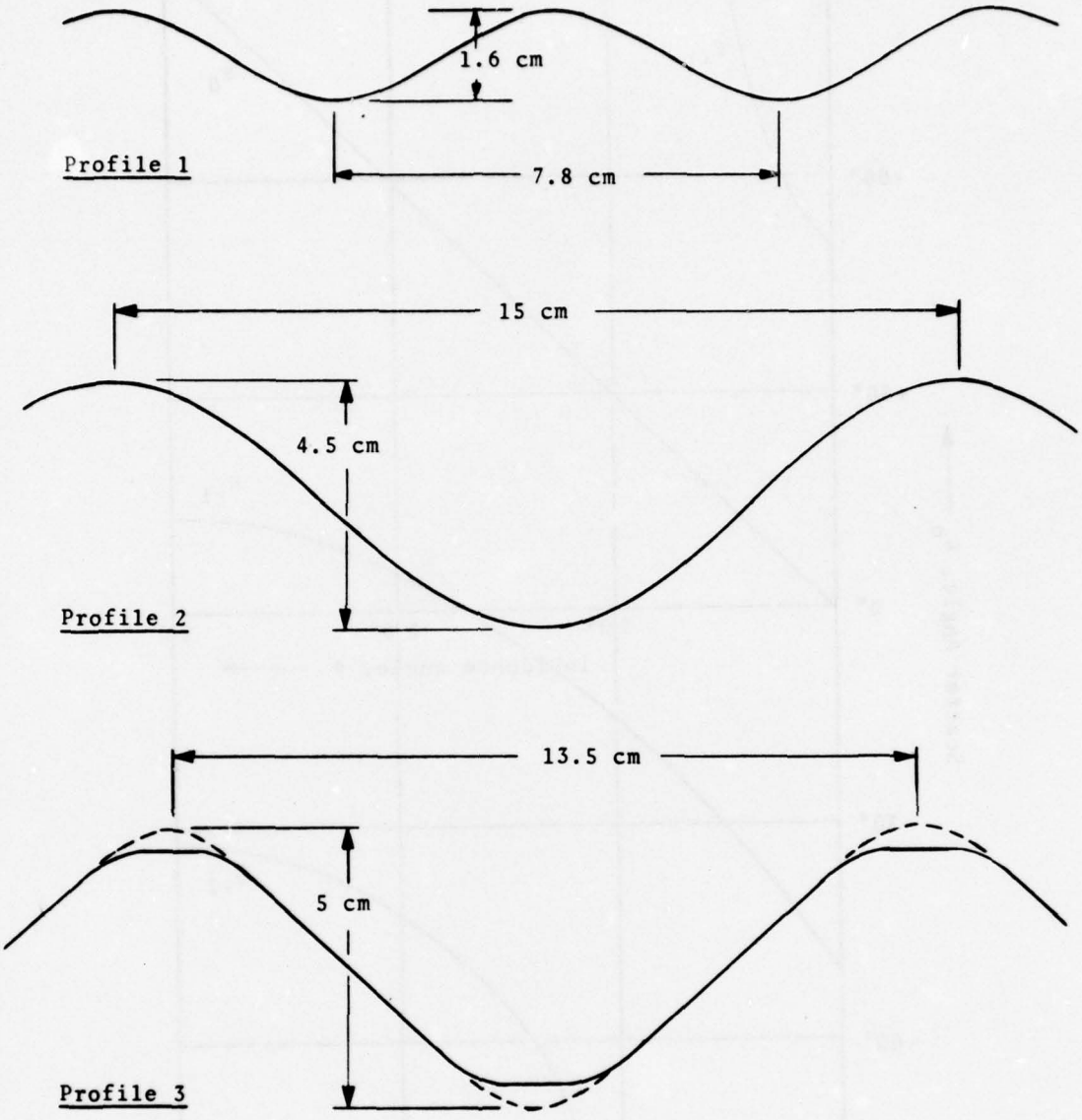

Fig. 2. *Traces of hangar-door profiles.* Numerical evaluation of periodic-surface scatter theory has been performed for these profiles assuming a wavelength of 6 cm (C-band).

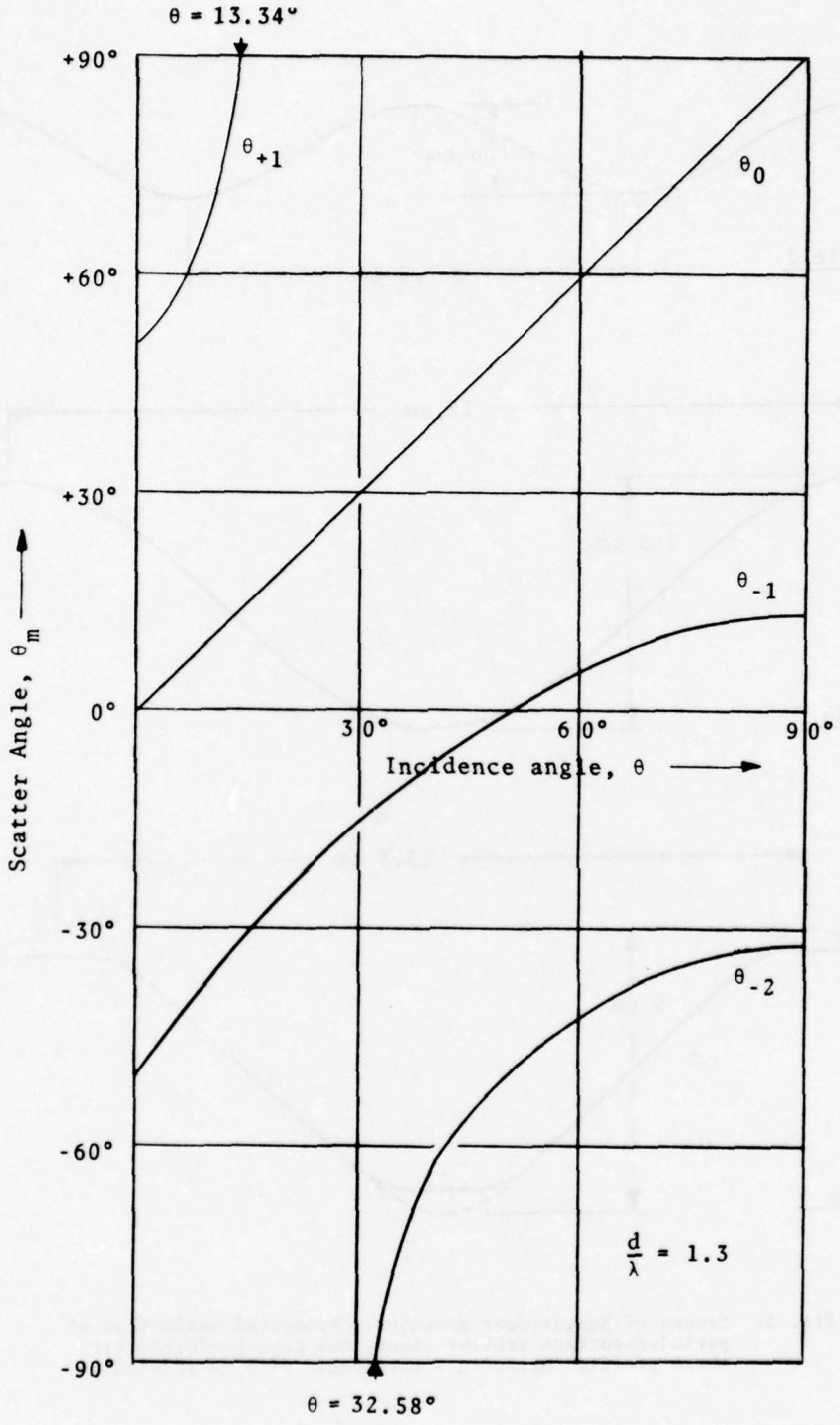

Fig. 3. Direction angles θ_m of propagating space harmonics of scatter field vs. arrival angle θ of incident plane wave (Profile 1).

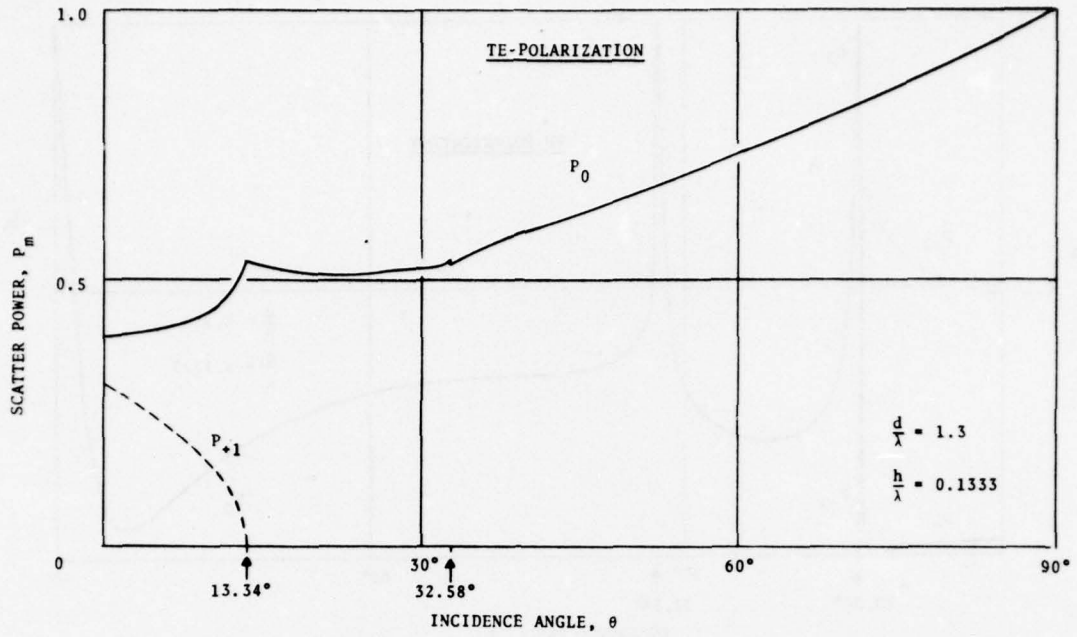

Fig. 4a. Powers P_m of propagating space harmonics vs. arrival angle θ of incident wave (Profile 1; Spectral orders: m = +1, 0).

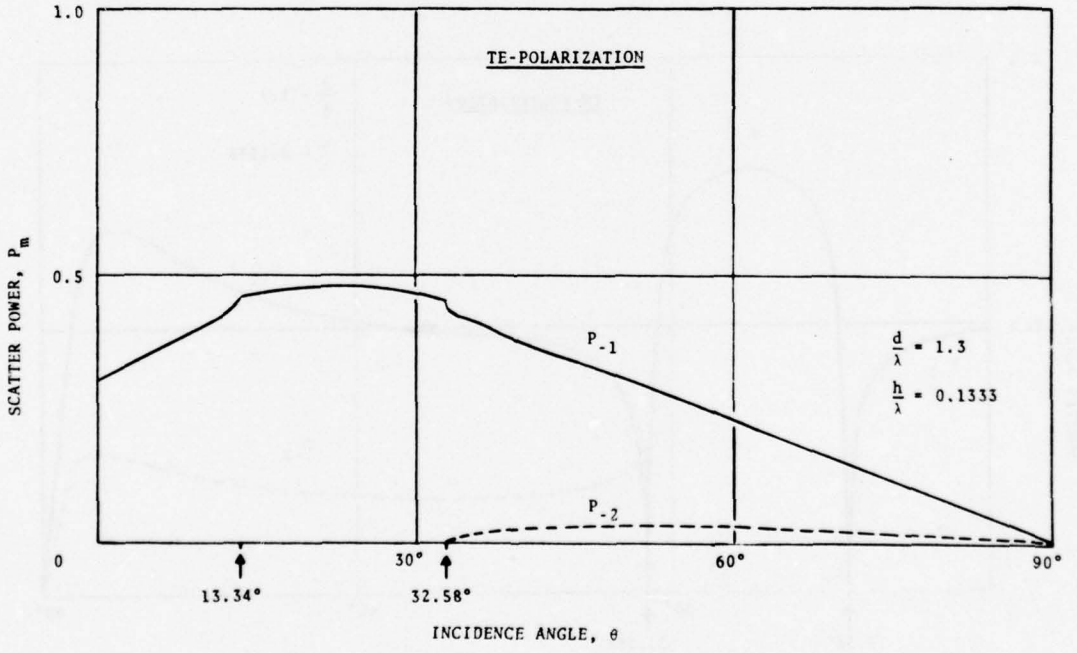

Fig. 4b. Powers P_m of propagating space harmonics vs. arrival angle θ of incident wave (Profile 1; Spectral orders: m = -1, -2).

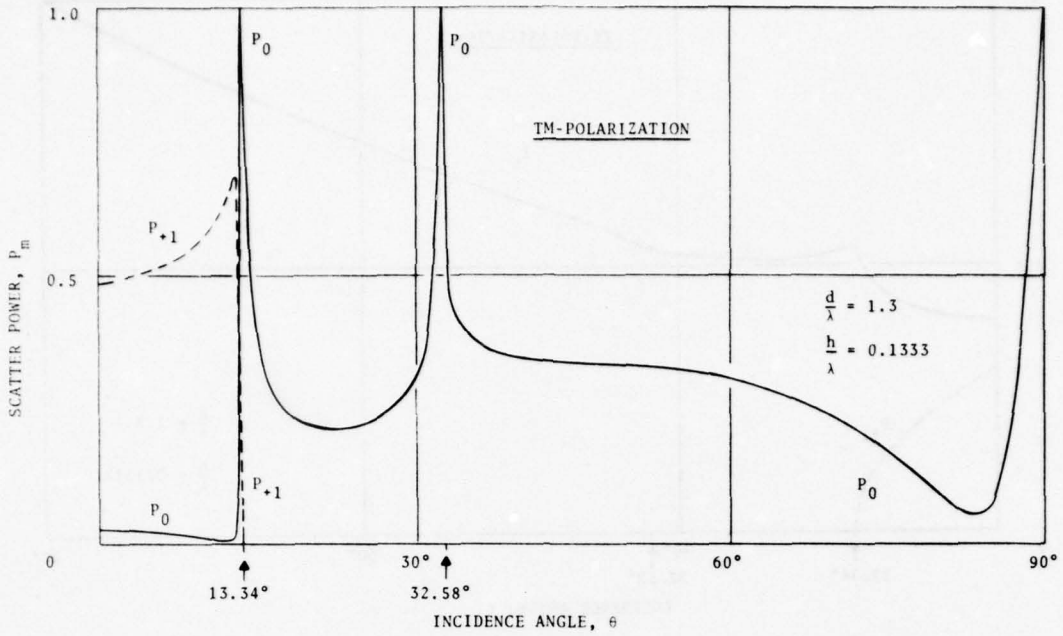

Fig. 5a. Powers P_m of propagating space harmonics vs. arrival angle θ of incident wave (Profile 1; Spectral orders: m = +1, 0).

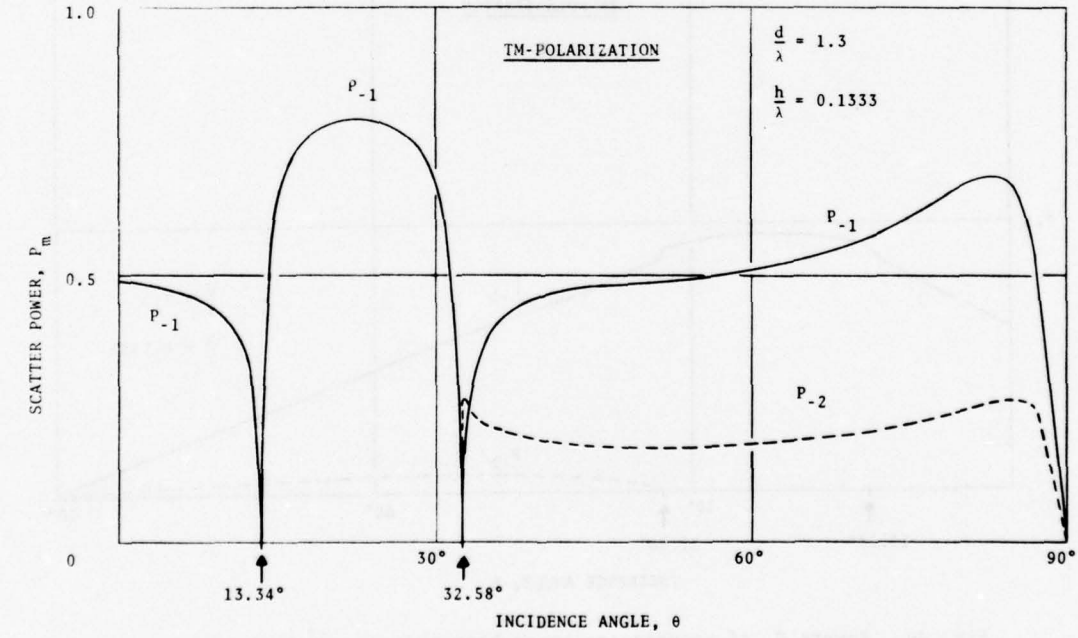

Fig. 5b. Powers P_m of propagating space harmonics vs. arrival angle θ of incident wave (Profile 1; Spectral orders: m = -1, -2).

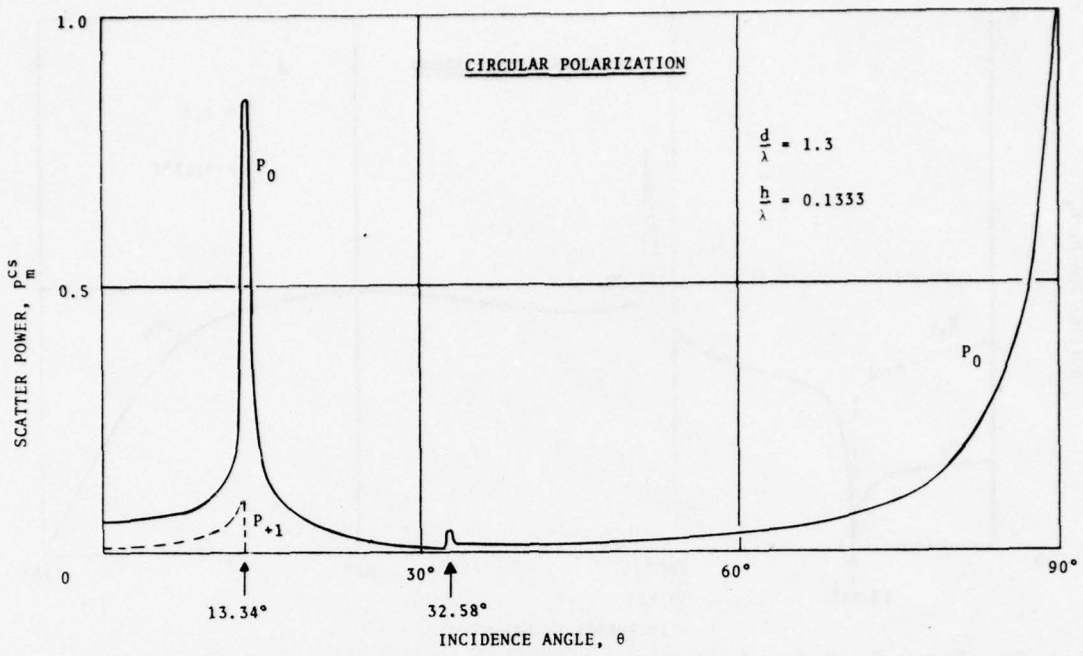

Fig. 6a. Powers P_m of propagating space harmonics vs. arrival angle θ of incident wave (Profile 1; Spectral orders: m = +1, 0; Polarization: Circular, with same sense of rotation as incident wave).

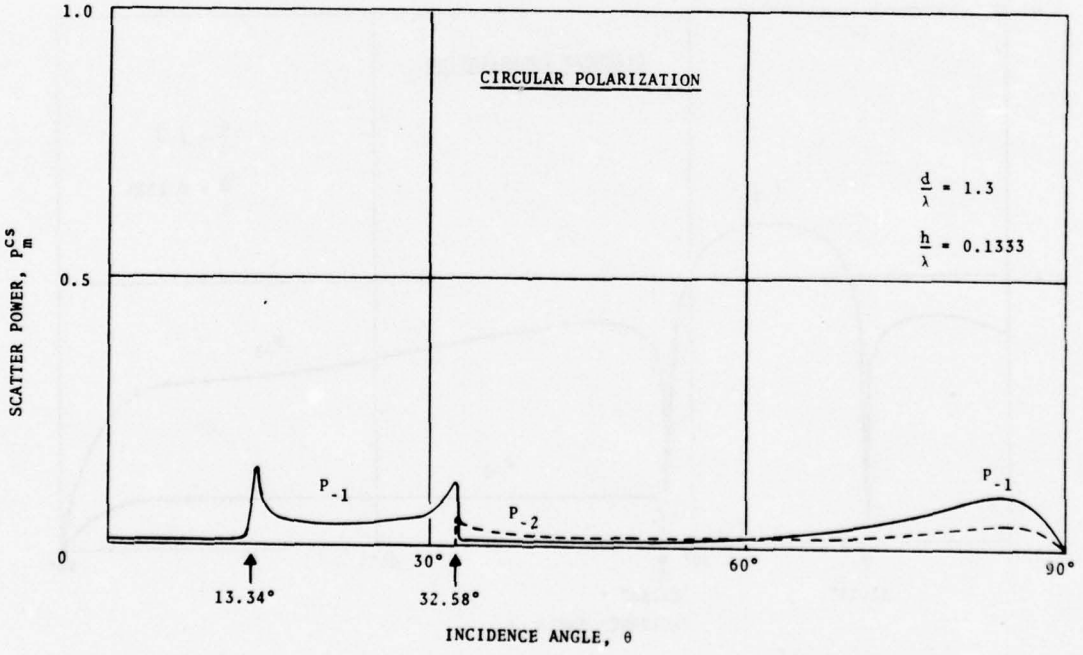

Fig. 6b. Powers P_m of propagating space harmonics vs. arrival angle θ of incident wave (Profile 1; Spectral orders: m = -1, -2; Polarization: Circular, with same sense of rotation as incident wave).

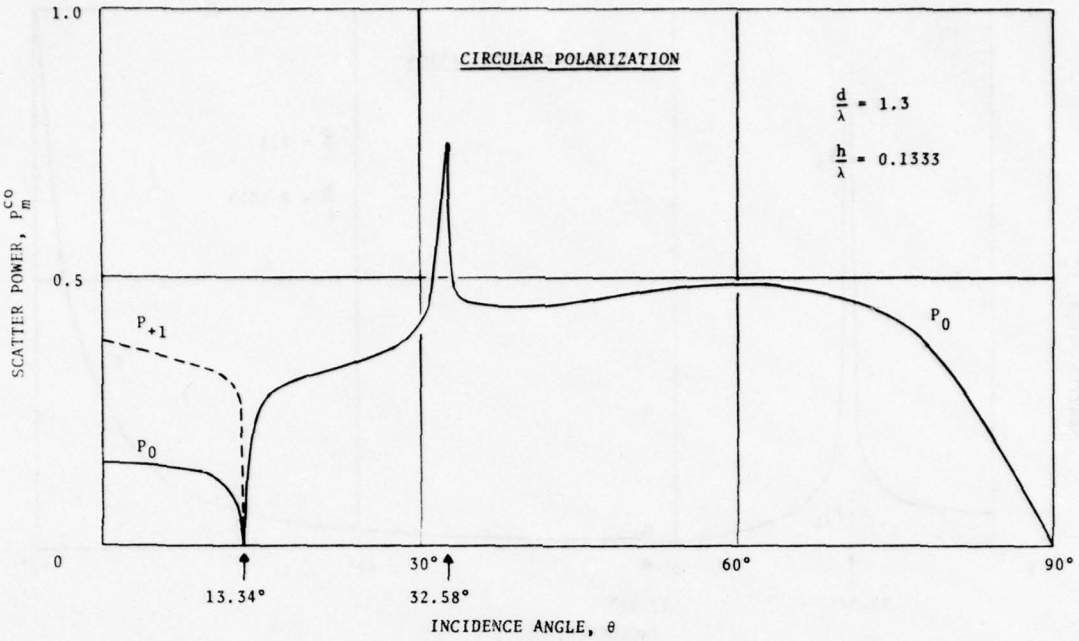

Fig. 7a. Powers P_m of propagating space harmonics vs. arrival angle θ of incident wave (Profile 1; Spectral orders: m = +1, 0; Polarization: Circular, with sense of rotation opposite to that of incident wave).

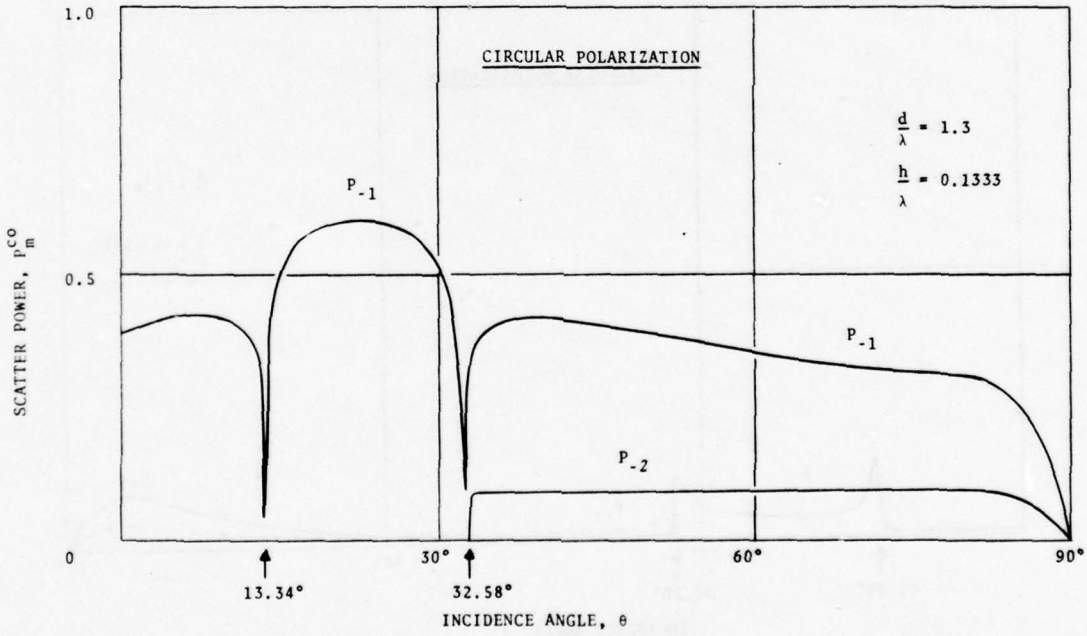

Fig. 7b. Powers P_m of propagating space harmonics vs. arrival angle θ of incident wave (Profile 1; Spectral orders: m = -1, -2; Polarization: Circular, with sense of rotation opposite to that of incident wave).

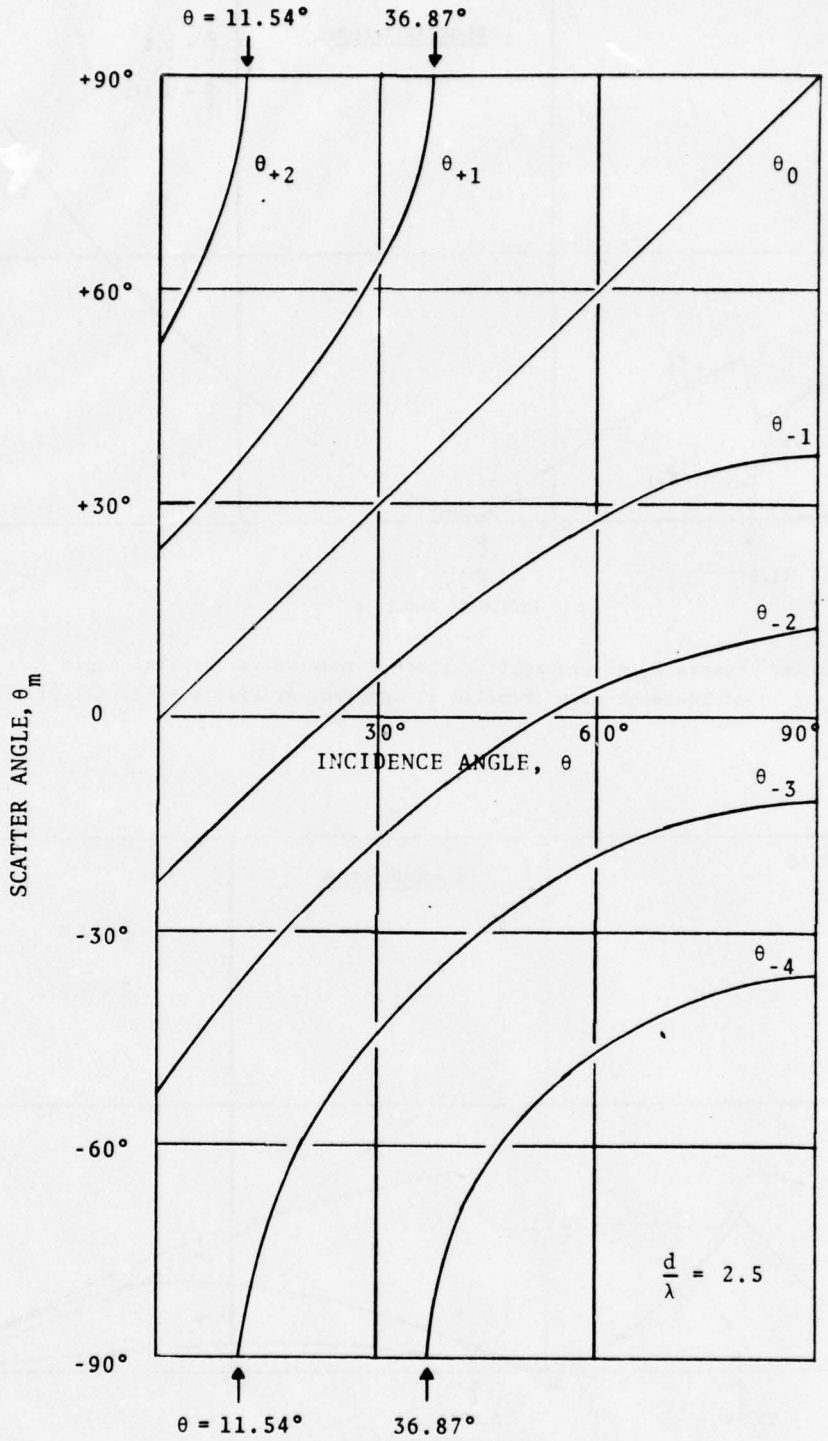

Fig. 8. Direction angles θ_m of propagating space harmonics of scatter field vs. arrival angle θ of incident plane wave (Profile 2).

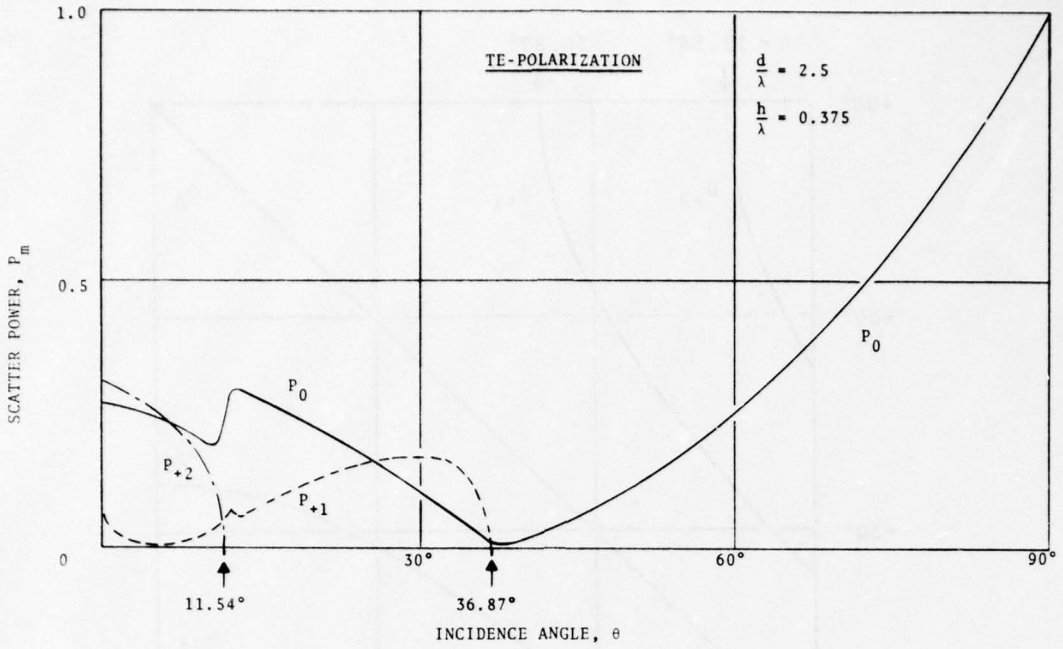

Fig. 9a. Powers P_m of propagating space harmonics vs. arrival angle θ of incident wave (Profile 2; Spectral orders: m = +2, +1, 0).

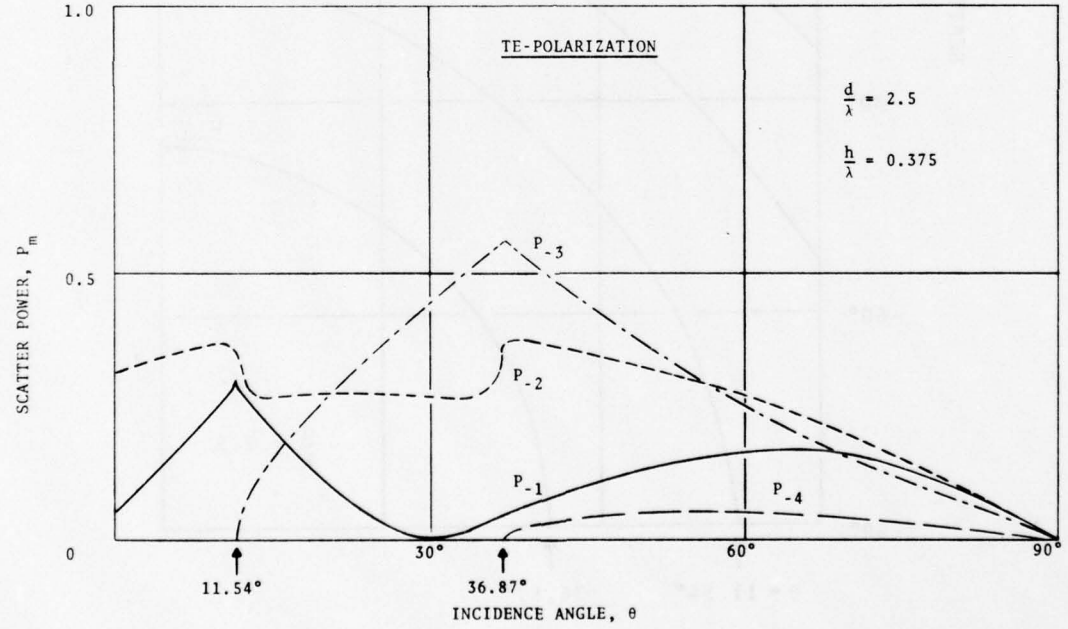

Fig. 9b. Powers P_m of propagating space harmonics vs. arrival angle θ of incident wave (Profile 2; Spectral orders: m = -1 through -4).

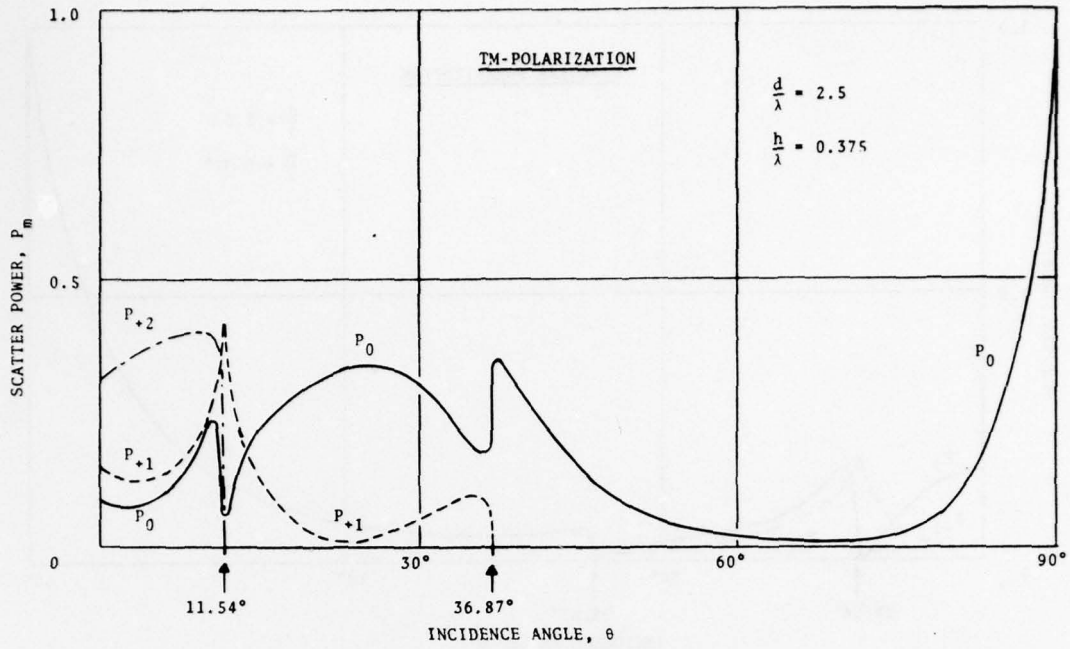

Fig. 10a. Powers P_m of propagating space harmonics vs. arrival angle θ of incident wave (Profile 2; Spectral orders: m = +2, +1, 0).

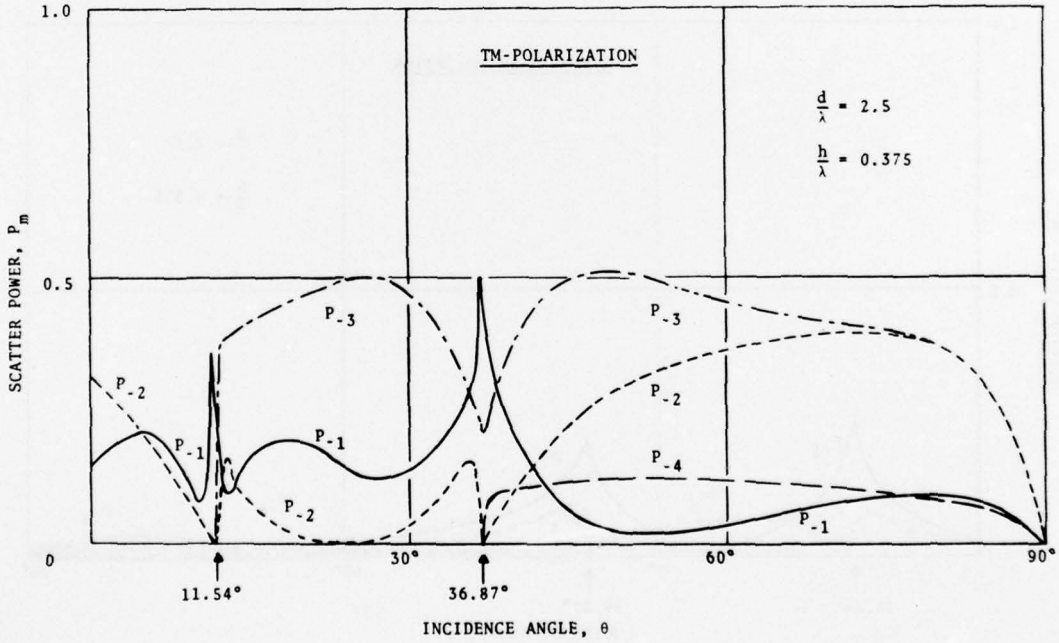

Fig. 10b. Powers P_m of propagating space harmonics vs. arrival angle θ of incident wave (Profile 2; Spectral orders: m = -1 through -4).

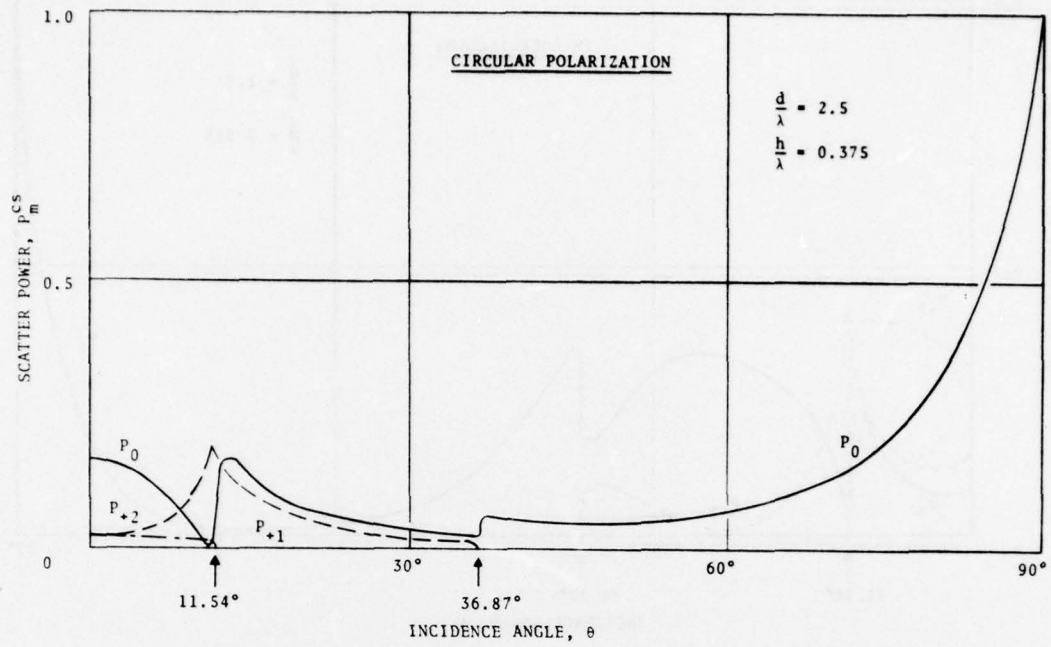

Fig. 11a. Powers P_m of propagating space harmonics vs. arrival angle θ of incident wave (Profile 2; Spectral orders: m = +2, +1, 0; Polarization: Circular, with same sense of rotation as incident wave).

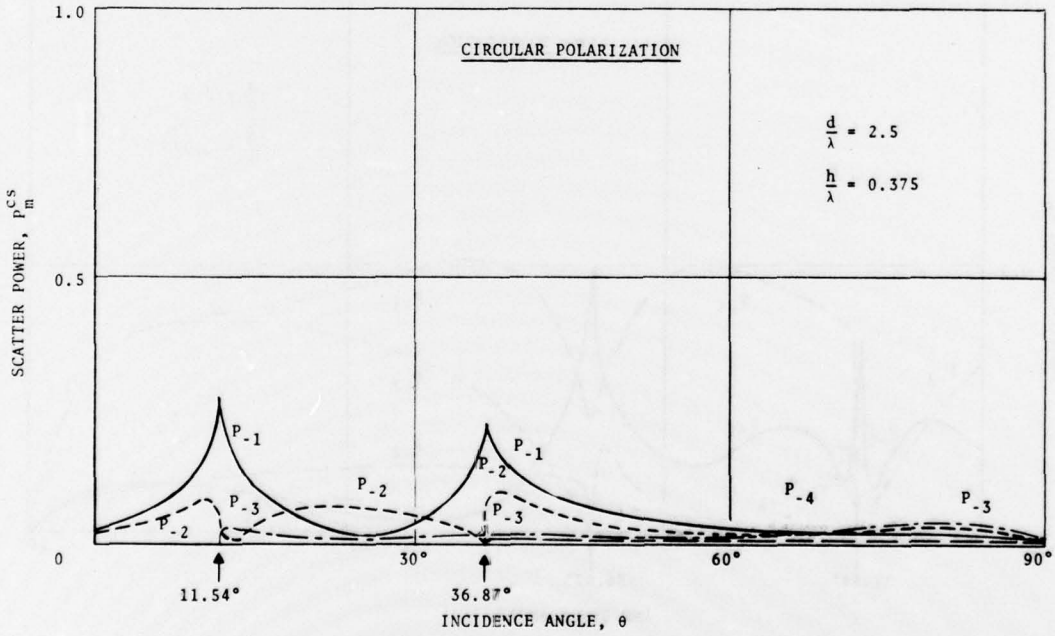

Fig. 11b. Powers P_m of propagating space harmonics vs. arrival angle θ of incident wave (Profile 2; Spectral orders: m = -1 through -4; Polarization: Circular, with same sense of rotation as incident wave).

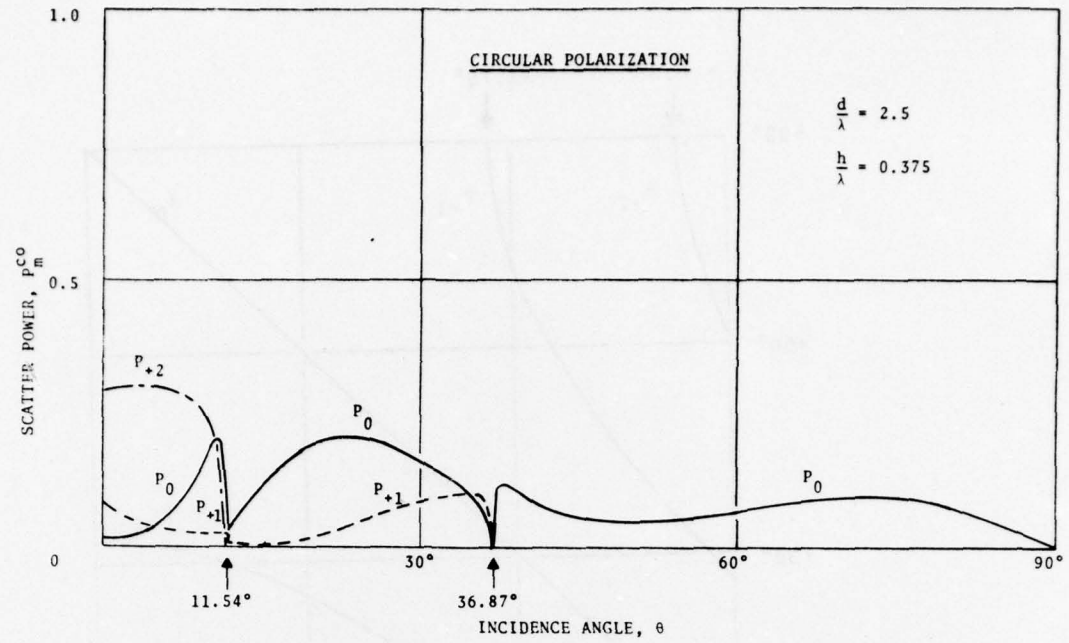

Fig. 12a. Powers P_m of propagating space harmonics vs. arrival angle θ of incident wave (Profile 2; Spectral orders: m = +2, +1, 0; Polarization: Circular, with sense of rotation opposite to that of incident wave).

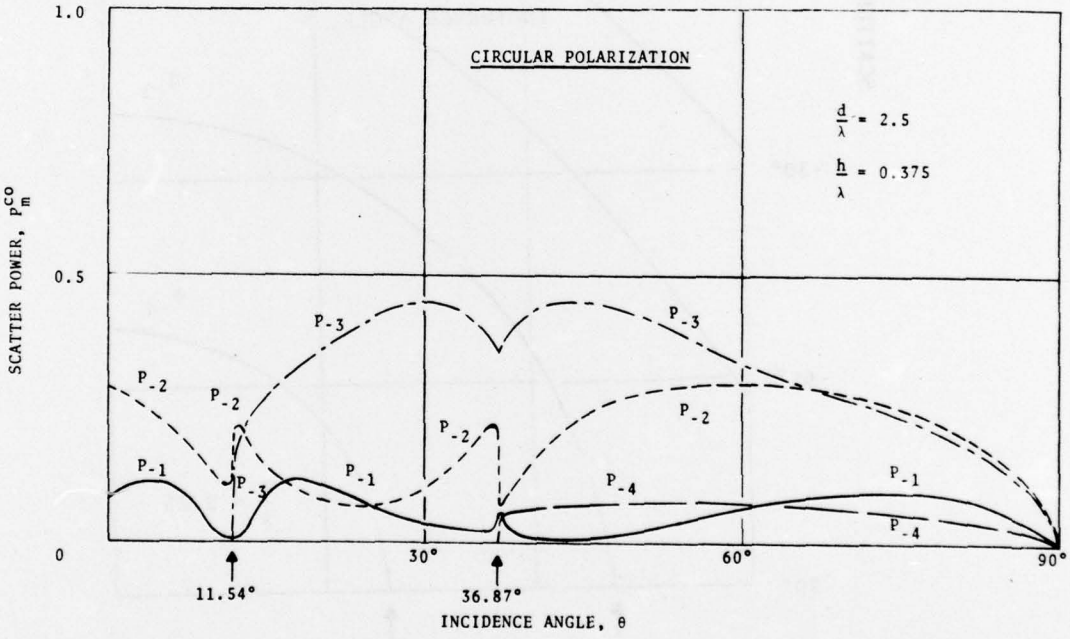

Fig. 12b. Powers P_m of propagating space harmonics vs. arrival angle θ of incident wave (Profile 2; Spectral orders: m = -1 through -4; Polarization: Circular, with sense of rotation opposite to that of incident wave).

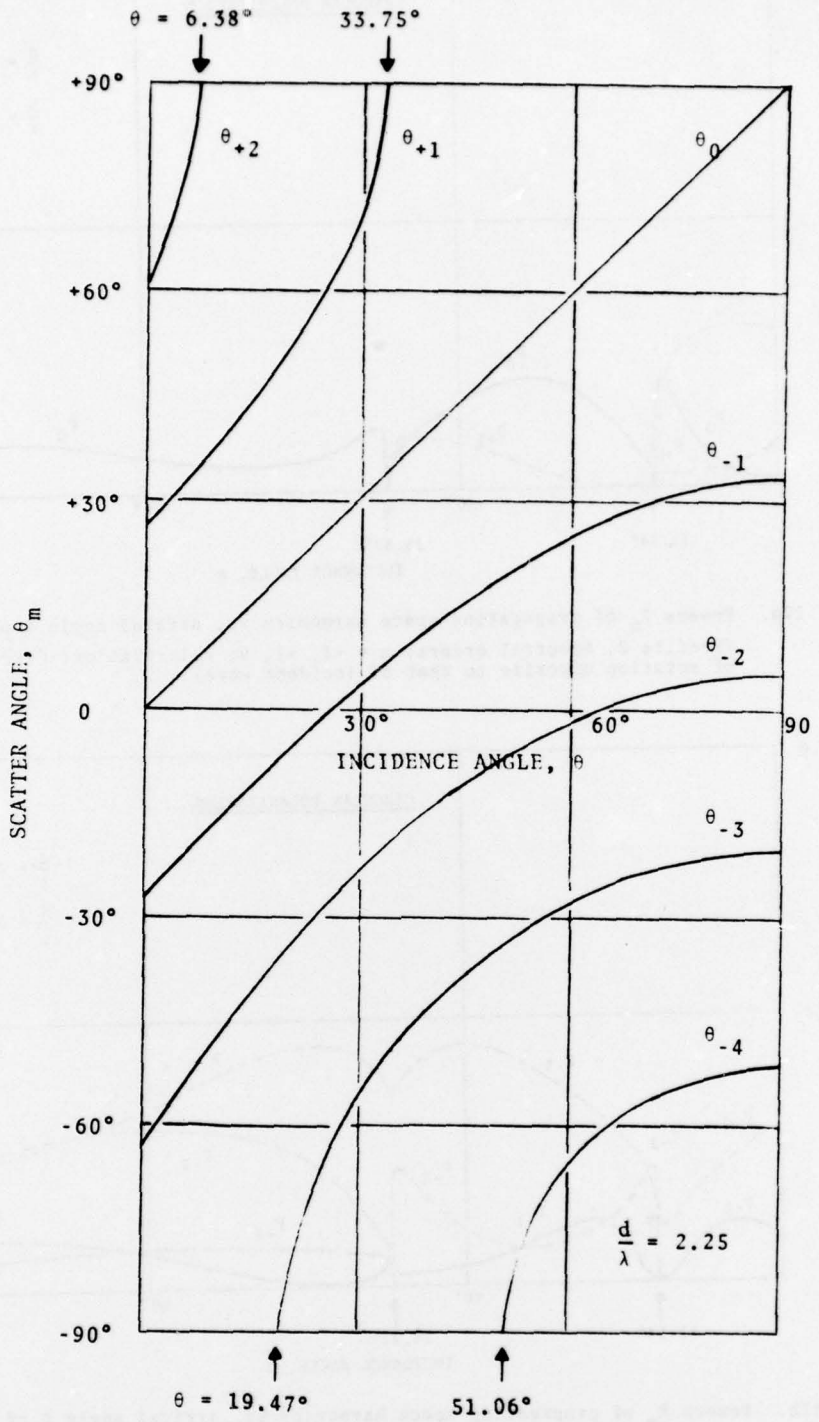

Fig. 13. Direction angles θ_m of propagating space harmonics of scatter field vs. arrival angle θ of incident plane wave (Profile 3).

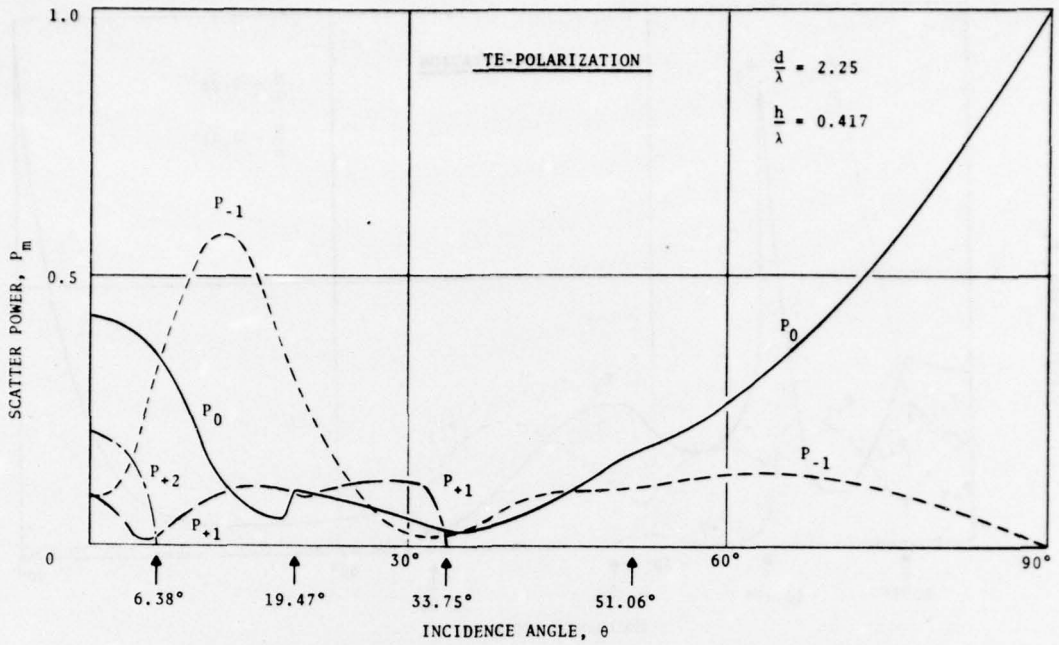

Fig. 14a. Powers P_m of propagating space harmonics vs. arrival angle θ of incident wave (Profile 3; Spectral orders: m = +2, +1, 0, -1).

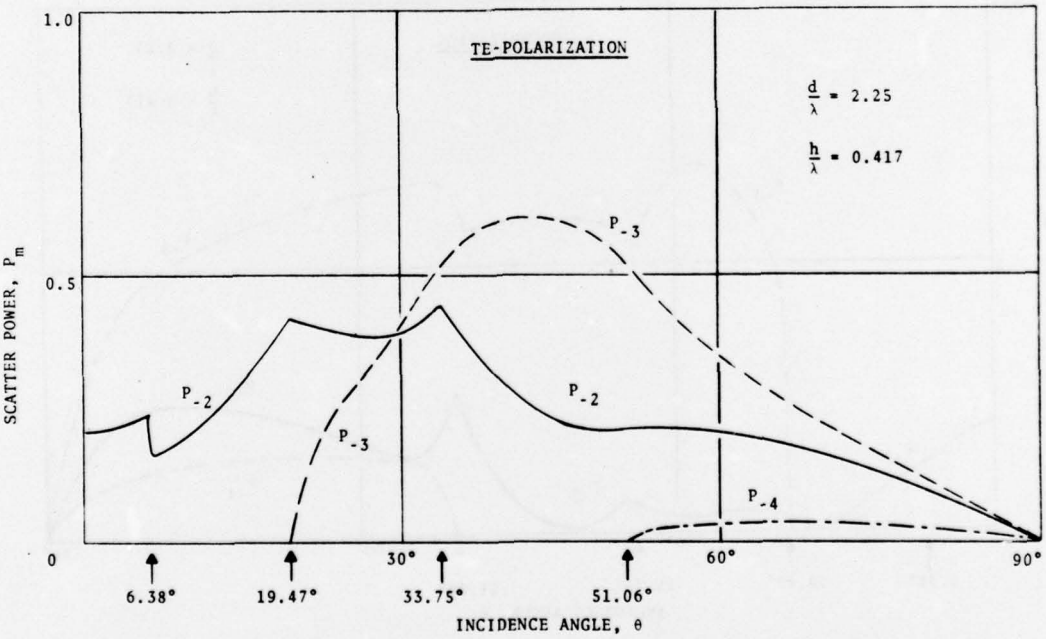

Fig. 14b. Powers P_m of propagating space harmonics vs. arrival angle θ of incident wave (Profile 3; Spectral orders: m = -2, -3, -4).

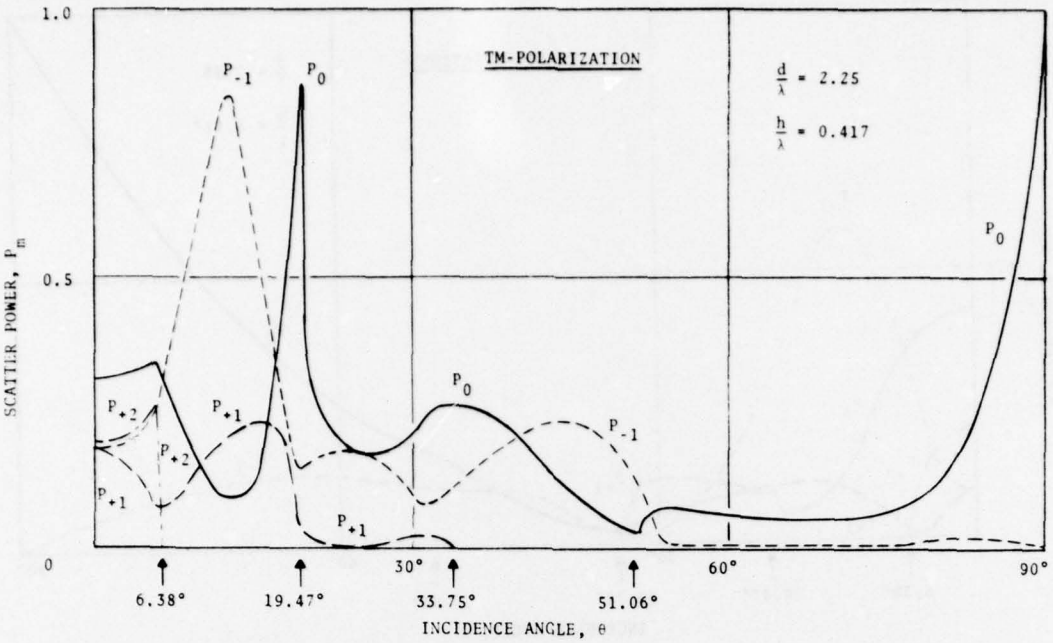

Fig. 15a. Powers P_m of propagating space harmonics vs. arrival angle θ of incident wave (Profile 3; Spectral orders: m = +2, +1, 0, -1).

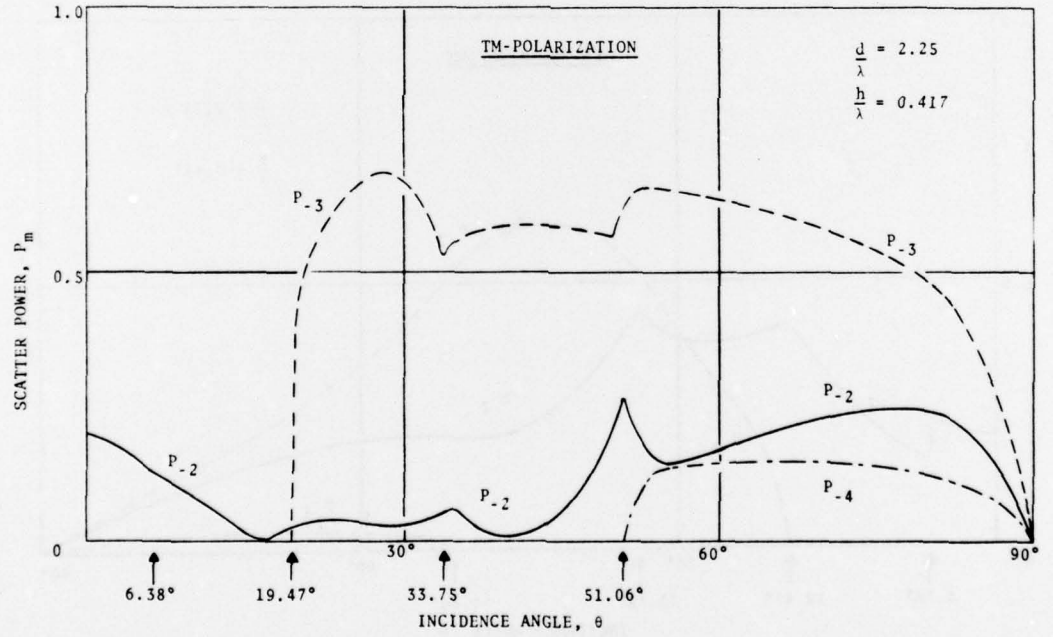

Fig. 15b. Powers P_m of propagating space harmonics vs. arrival angle θ of incident wave (Profile 3; Spectral orders: m = -2, -3, -4).

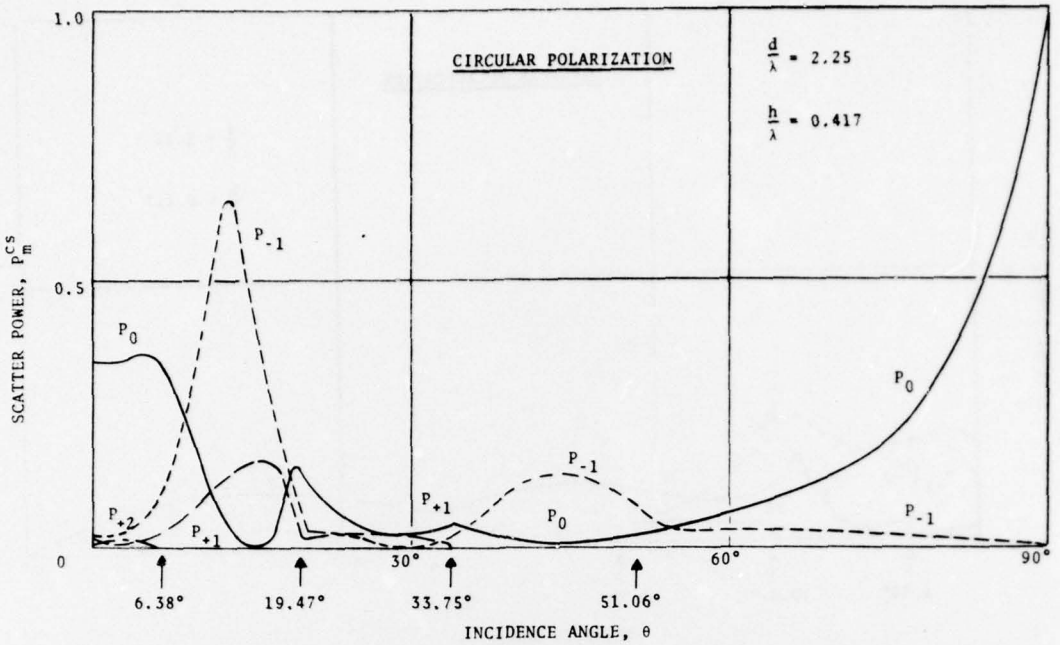

Fig. 16a. Powers P_m of propagating space harmonics vs. arrival angle θ of incident wave (Profile 3; Spectral orders: m = +2, +1, 0, -1; Polarization: Circular, with same sense of rotation as incident wave).

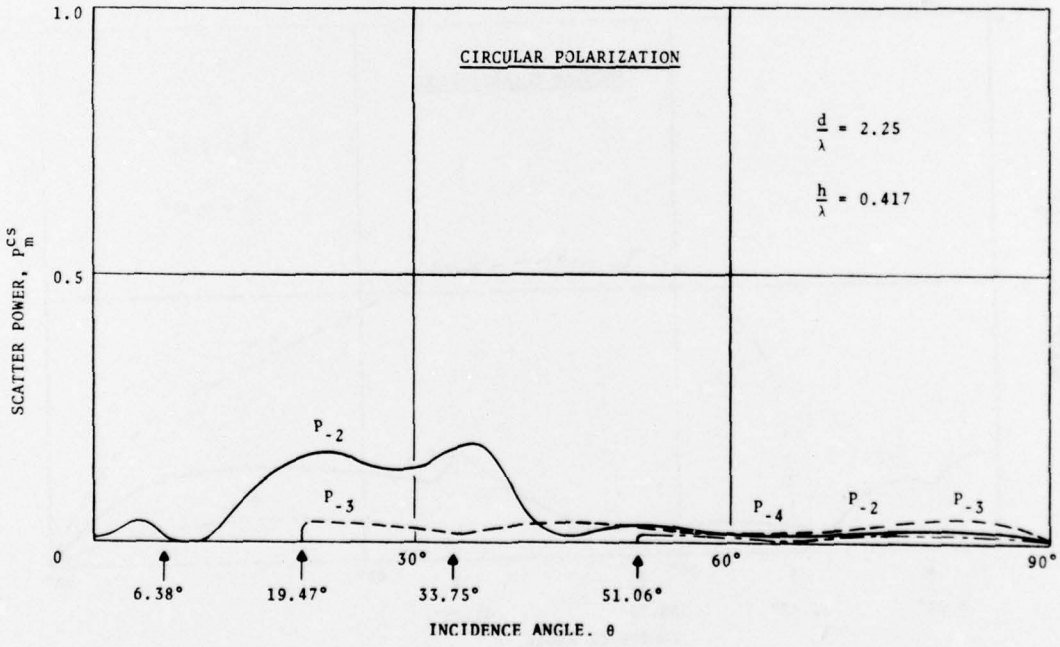

Fig. 16b. Powers P_m of propagating space harmonics vs. arrival angle θ of incident wave (Profile 3; Spectral orders: m = -2, -3, -4; Polarization: Circular, with same sense of rotation as incident wave).

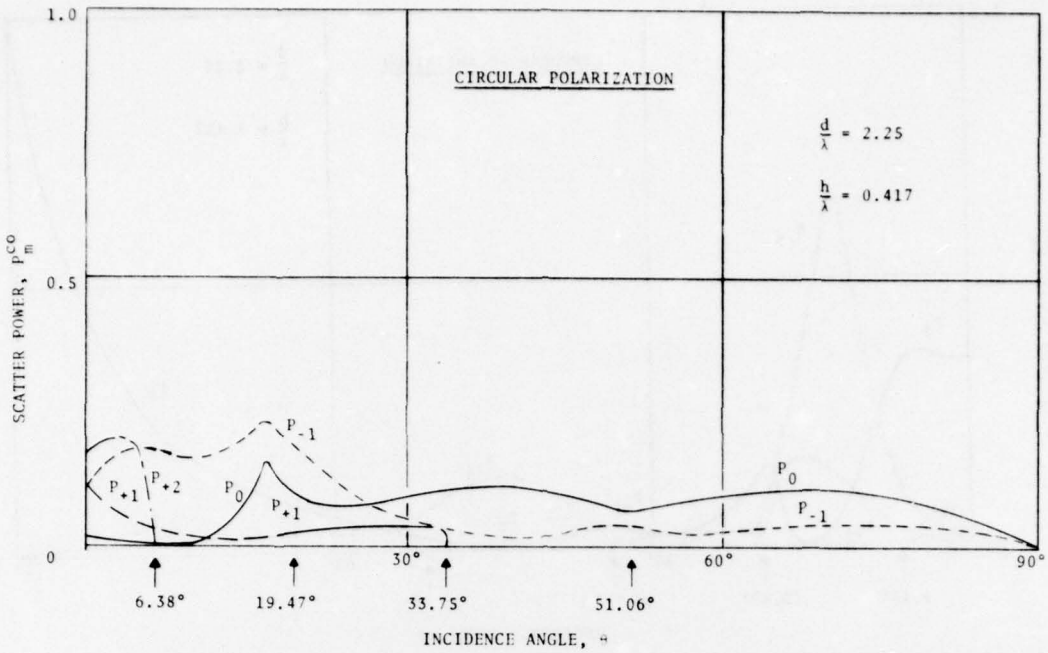

Fig. 17a. Powers P_m of propagating space harmonics vs. arrival angle θ of incident wave (Profile 3; Spectral orders: m = +2, +1, 0, -1; Polarization: Circular, with sense of rotation opposite to that of incident wave).

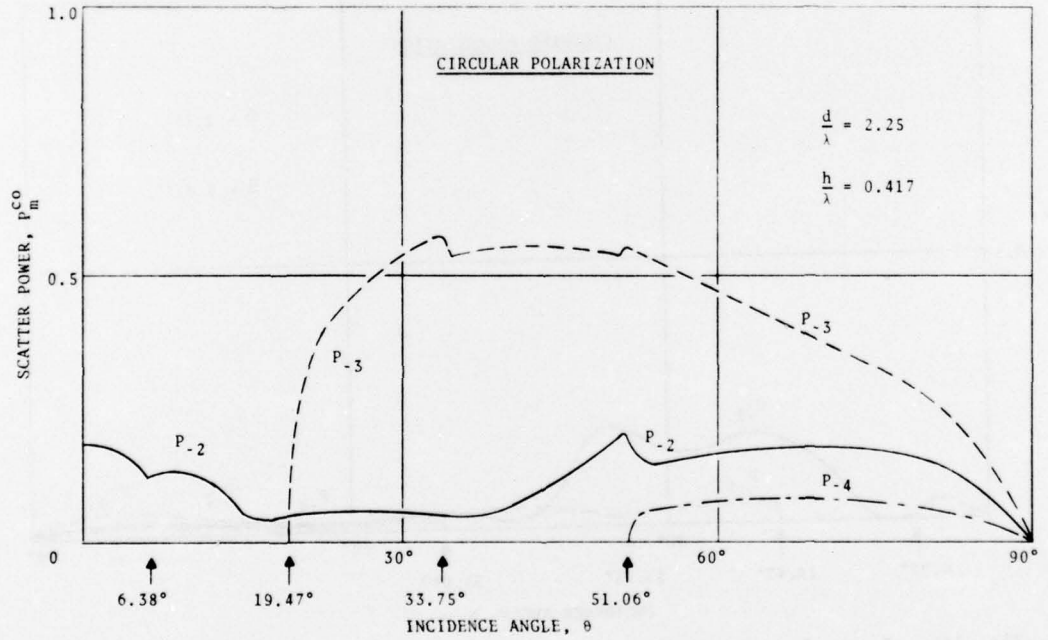

Fig. 17b. Powers P_m of propagating space harmonics vs. arrival angle θ of incident wave (Profile 3; Spectral orders: m = -2, -3, -4; Polarization: Circular, with sense of rotation opposite to that of incident wave).

$$P_m = \begin{cases} \dfrac{E_m \cdot E_m^* \cos\theta_m}{E^P \cdot E^{P*} \cos\theta} & \text{for TE-polarization} \quad (19a) \\ \dfrac{H_m \cdot H_m^* \cos\theta_m}{\frac{\epsilon}{\mu} E^P \cdot E^{P*} \cos\theta} & \text{for TM-polarization .} \quad (19b) \end{cases}$$

In the case of circular polarization, the power of each space harmonic is split into two (orthogonal) contributions:

$$P_m^{CS} = \frac{E_m^{CS} \cdot E_m^{CS*} \cos\theta_m}{E^P \cdot E^{P*} \cos\theta} \quad (19c)$$

and

$$P_m^{CO} = \frac{E_m^{CO} \cdot E_m^{CO*} \cos\theta_m}{E^P \cdot E^{P*} \cos\theta} , \quad (19d)$$

which correspond to circularly polarized waves having the same and the opposite sense of rotation as the incident wave.

It is apparent from the P_m vs. θ curves that the specular reflection coefficient (P_0) is significantly smaller for TM- than for TE-polarization, particularly in the range of large incidence angles $\theta > 60^\circ$. Hence, the choice of horizontal polarization over vertical polarization for microwave landing systems will significantly reduce the probability of false guidance caused by specular reflection from large periodic metal surfaces near runways. (It is assumed here that the grooves of the surfaces run in the vertical direction.) One of the objectives of the present study was to confirm this experimentally-observed effect theoretically. However, when P_0 is small, one of the higher order space harmonics may become dominant and carry a major portion of the incident power. Observe, for example, spectral orders m = -1 for Profile 1 (Fig. 5b) and m = -3 for Profile 3. In the latter case, the dominant space harmonic is more or less backscattered and therefore not likely to cause false guidance by microwave landing systems; see Fig. 13. At angles very close to grazing incidence, $\theta \to 90^\circ$, the specular reflection coefficient, of course, approaches unity for TM- as well as for TE-polarization.

For all three profiles considered here, circular polarization is very effective in suppressing higher order space harmonics having the same polarization (same sense of rotation) as the incident wave. Higher order space harmonics of opposite rotational sense are present with significant amplitudes; however, they could not be received by an airborne antenna polarized to receive the primary microwave beam.

All power curves show Rayleigh-type Wood anomalies. Near those angles of incidence θ where particular space harmonics are at grazing angles (and thus change their character from propagating to evanescent or vice versa), the power distribution over the remaining propagating space harmonics is reordered rapidly, which results in steep peaks or valleys in the power curves [8]. These anomalies are pronounced in the case of TM- and weaker for TE-polarization, an effect discussed in detail in the literature on optical gratings. The condition for Wood anomalies to occur is $\theta_m = \pm 90^\circ$; hence with Eq. (4)

$$\theta = \sin^{-1} \left(\pm 1 - m \frac{\lambda}{d} \right) .$$

These incidence angles are indicated in the figures by small arrows. Note that both anomalies of Profile 2 are double anomalies (two space harmonics at grazing angles simultaneously); therefore a particularly strong effect should be expected.

5. NUMERICAL ACCURACY AND LIMITATIONS OF PROGRAM

Two criteria were used to check the accuracy of numerical results: a power criterion and a reciprocity criterion.

Conservation of power requires that

$$\sum_{m_1}^{m_2} P_m = 1 \qquad (20a)$$

for TE- and TM-polarization, and that

$$\sum_{m_1}^{m_2} \left(P_m^{CS} + P_m^{CO} \right) = 1 \qquad (20b)$$

---

[8] The curves for Profile 3 were drawn using data points at θ intervals of 5°. Therefore, a certain amount of conjecturing was required near anomalies, and the curves may not be accurate. In plotting the curves for Profiles 1 and 2, data points at 0.5°-intervals were used near anomalies. These curves should be reliable.

for circular polarization; the summations extend over all propagating spectral orders. In general, it has been found that criterion (20a) is satisfied with higher accuracy for TE- than for TM-polarization; but exceptions are not uncommon. The relative error, i.e., the deviation of the left-hand side of Eq. (20a) from unity, is typically in the order of 1% or less for Profiles 2 and 3, although in a few cases larger errors occur for TM-polarization. For Profile 1, the accuracy is very high, the error being in the order of 10^{-4} %.

The reciprocity theorem applied to the problem of scattering by periodic surfaces leads to the following observations. Consider two plane waves incident from directions θ^a and θ^b. If the first of these waves scatters a space harmonic (of order m) into the direction of the second, such that $\theta_m^a = -\theta^b$, then the second wave generates a space harmonic of the same spectral order m propagating in the direction of the first incident wave; hence $\theta_m^b = -\theta^a$ [9] and the complex amplitudes of the two space harmonics are related by:

$$E_m^a \cos\theta_m^a = E_m^b \cos\theta_m^b \tag{21a}$$

and

$$H_m^a \cos\theta_m^a = H_m^b \cos\theta_m^b \tag{21b}$$

where the first equation is used in the TE case and the second in the TM case. We have assumed that the incident waves have equal amplitude and phase.

Criteria (20a) and (21) supplement each other. The former criterion checks on the accumulated power of all propagating space harmonics, the latter criterion provides a check on amplitude and phase of individual space harmonics. In general, it has been observed that when the power criterion is well satisfied (within 1% or better), the same is true for the reciprocity criterion.

The accuracy of the numerical results has been found to be critically dependent on the groove depth 2h. When this depth is less than one wavelength, the accuracy as measured by the power and reciprocity criteria is, in general, acceptable; when $2h \ll \lambda$, the accuracy is excellent. However, when 2h approaches or exceeds λ, the accuracy sooner or later breaks down and unacceptable errors result. It has not yet been determined whether

---

[9] With regard to the minus signs in the relations $\theta_m^a = -\theta^b$ and $\theta_m^b = -\theta^a$, see footnote [7] on page 12.

this limitation is due to poor convergence of the linear systems (13a) and (13b) at large h,or if it is caused by subroutines used in the program (such as the one used for computing Bessel functions of complex arguments).

With respect to groove width d, no limitation of the program has been encountered. Accuracy tends to increase, rather than decrease, with d. This is to be expected since the underlying analytical method is basically an extension of the physical optics approximation.

As an additional check, the above program was tested against an existing program developed by Zaki and Neureuther [10], [11]. Their program is based on a theory which uses a Green's function to derive an inhomogeneous integral equation for the current distribution on the metal surface. From the current distribution, the amplitudes of the space harmonics are computed. This integral equation is solved numerically, assuming--as in the present theory--a sinusoidal height profile. Because of high computational cost, comparison of the two programs had to be limited to a small set of parameter values, namely,

$$\theta = 0^\circ \text{ and } 60^\circ$$

$$d/\lambda = 1.5,\ 2.5, \text{ and } 3.5$$

$$h/\lambda = 0.1 \text{ and } 0.25.$$

Hence, the comparison must be considered preliminary. However, the powers P_m of the propagating space harmonics calculated with these programs were found to be in excellent agreement for each parameter set.

In Table 2, the relative error according to the power criterion (20b)

$$\varepsilon = \left|1 - \sum_m P_m\right| \cdot 100\% ,$$

is given together with the computation time T for each run [12]. For the small surface depths considered, the accuracy of the new program (W-S),

---

[10] K. A. Zaki and A. R. Neureuther, "Scattering from a perfectly conducting surface with a sinusoidal height profile: TE-polarization," IEEE Trans. Antennas & Progagation, vol. AP-19, March 1971, pp. 208-214.

[11] _____, "Scattering from a perfectly conducting surface with a sinusoidal height profile: TM-polarization," IEEE Trans. Antennas & Propagation, vol. AP-19, November 1971, pp. 747-751.

[12] The programs were run on a Burrough's B-5500 Computer.

Table 2. Comparison of Whitman-Schwering (W-S) Program and Zaki-Neureuther (Z-N) Program Concerning Relative Error (according to power criterion) and Computation Time.

Surface Parameters		Incidence Angles	Relative Error ε in Percent				Computation Time T in seconds			
			TE-Polarization		TM-Polarization		TE-Polarization		TM-Polarization	
d/λ	h/λ	θ (degrees)	W-S	Z-N	W-S	Z-N	W-S	Z-N	W-S	Z-N
1.5	0.1	0	10^{-5}	$0.60 \cdot 10^{-2}$	$0.77 \cdot 10^{-5}$	0.13		193		197
2.5			$0.93 \cdot 10^{-7}$	$0.25 \cdot 10^{-2}$	$0.69 \cdot 10^{-7}$	10^{-2}		742		768
3.5			$0.73 \cdot 10^{-9}$	$0.38 \cdot 10^{-2}$	$0.27 \cdot 10^{-8}$	$0.41 \cdot 10^{-2}$		1399		1417
1.5	0.1	60	$0.44 \cdot 10^{-4}$	$0.69 \cdot 10^{-2}$	$0.46 \cdot 10^{-4}$	1.18		188		240
2.5			$0.44 \cdot 10^{-4}$	$0.15 \cdot 10^{-3}$	$0.21 \cdot 10^{-4}$	0.78		828		1072
3.5			$0.40 \cdot 10^{-4}$	$0.33 \cdot 10^{-3}$	$0.29 \cdot 10^{-5}$	1.31		1441		2016
				Subtotal of Computation Time			440	4791	440	5710
1.5	0.25	0	$1.18 \cdot 10^{-2}$	$1.77 \cdot 10^{-2}$	0.12	0.60		283		368
2.5			$0.30 \cdot 10^{-4}$	$0.26 \cdot 10^{-2}$	$1.42 \cdot 10^{-5}$	$0.93 \cdot 10^{-1}$		624		647
3.5			$0.85 \cdot 10^{-6}$	$0.41 \cdot 10^{-2}$	$1.61 \cdot 10^{-6}$	$0.42 \cdot 10^{-1}$		1072		1288
1.5	0.25	60	$0.82 \cdot 10^{-3}$	$1.72 \cdot 10^{-2}$	$0.55 \cdot 10^{-2}$	0.23		324		406
2.5			0.23	$0.16 \cdot 10^{-2}$	0.27	0.57		703		941
3.5			3.07	$0.34 \cdot 10^{-2}$	4.14	1.16		1317		1647
				Subtotal of Computation Time			445	4323	445	5297
				Total Computation Time			885	9114	885	11,007

in general, exceeds that of the existing program (Z-N), which, however, is fully sufficient for all practical purposes. With increasing h/λ, the relative accuracy of the two programs is expected to invert: the Z-N program is probably usable at h/λ values substantially in excess of 0.5, the practical limit of the W-S program at least in its present form.

The computation time of the W-S program is more or less independent of surface parameters and incidence angle; therefore, only the total running time is presented. The average time per run is $\tilde{\sim}$ 75 sec. In contrast, the computation time of the Z-N program increases substantially with d/λ. If the parameter values of Table 2 are used as a basis for comparison, the W-S program runs, on the average, $\tilde{\sim}$ 10 times faster than the Z-N program. This conclusion, however, should be regarded with caution, since it is based on a small sample of test cases. Moreover, the d/λ values considered here are comparatively large; at smaller d/λ values the running times of the two programs compare more favorably. It should also be noted that the Z-N program includes evaluation of the physical optics approximation, which is not considered in the W-S program.

6. CONCLUSIONS AND RECOMMENDATIONS

(a) A rigorous theoretical approach to the problem of scattering by periodic metal surfaces has been discussed. This theory reduces the scatter problem to the familiar task of solving a system of linear equations. In the case considered here, the periodic surface has a sinusoidal height profile and the coefficients of the linear system are obtained as closed form expressions in terms of Bessel functions. The theory is amenable to efficient computer evaluation.

(b) A second class of periodic surfaces which can be handled efficiently by the new approach is comprised of those having piecewise linear height profiles. The coefficient matrices of the corresponding linear systems reduce to closed form expressions in terms of exponential functions. A theory for trapezoidal surfaces is already available and has been programmed for computer evaluation at the New Jersey Institute of Technology. Evaluation is in progress.

(c) Numerical evaluations performed for sinusoidal surfaces with periods of the order of a wavelength show that the specular reflection coefficient of such surfaces is significantly smaller for TM- than for TE-polarization, particularly in the range of incidence angles $\theta > 60^{\circ}$. At grazing incidence, $\theta = 90^{\circ}$, the specular reflection coefficient, of course, is unity for both cases.

(d) Circular polarization was found to be highly effective in suppressing higher order grating lobes of the same polarization as the incident wave. Grating lobes circularly polarized with a rotational sense opposite to that

of the incident wave, however, are present with significant amplitudes.

(e) The accuracy of the W-S computer program is critically dependent on groove depth. Further work is required to extend the applicability of this program to groove depths of more than one wavelength, which is the present limitation. With respect to groove width, no limitation of the program has been encountered (evaluations have been performed for groove widths up to 10 λ).

(f) A systematic comparison of the new program with the Zaki and Neureuther program and other existing codes (as for example, the Tong and Senior program) is recommended.

(g) Experiments to verify theoretical results have been conducted at ECOM. These experiments were designed and conducted by Dr. J. Mink [13]. In general, good agreement between theory and experiment was obtained, although in a few cases--at angles of incidence near grazing--substantial discrepancies were observed.

7. ACKNOWLEDGMENTS

The authors wish to thank Mrs. H. Perlman for writing the computer program and Mr. L. Leskowitz of the ECOM Math. Analysis Section for assistance in adapting existing programs to computers at ECOM. Thanks are extended to Messrs. P. Demko and R. Boriss of Avionics Laboratory for their continued interest in this study. Thanks are due Drs. G. Goubau and J. Mink for helpful discussions. The authors are grateful to Dr. Zaki of the University of Maryland and Dr. Neureuther of the University of California for making their program available to us.

This study was conducted jointly by the Communications/Automatic Data Processing Laboratory, ECOM, and the New Jersey Institute of Technology during the summers of 1973 and 1974. During these periods, Dr. G. Whitman, the co-author of this report, worked with the Antenna Team of the Communications/Automatic Data Processing Lab., under the Laboratory Research Cooperative Program.

---

[13] J. W. Mink, "Energy considerations of beams reflected from periodic surfaces," Communications/ADP Lab. Technical Memorandum, 29 August 1975.